博士論文

Analysis of Rab small GTPases that regulate primary ciliogenesis
（一次繊毛形成を制御する低分子量 G タンパク質 Rab の同定と機能解析）

令和２年度
東北大学大学院生命科学研究科
脳生命統御科学専攻
小口　舞

Contents

Abbreviations

AA, amino acid(s)

bsr, blasticidin S-resistant gene

EGFP, enhanced green fluorescent protein

FLCN, Folliculin

HRP, horseradish peroxidase

hTERT-RPE1, human telomerase reverse transcriptase retinal pigment epithelium 1

KC/AA, K115A/C116A

KD, knockdown

KO, knockout

puro, puromycin-resistant gene

MDCK, Madin-Darby canine kidney

NS, not significant

RILP, Rab interacting lysosomal protein

RILP-L1/L2, RILP-like 1/2

SR, siRNA-resistant

Abstract

Primary cilia are sensors of chemical and mechanical signals in the extracellular environment. The formation of primary cilia (i.e., ciliogenesis) requires dynamic membrane trafficking events, and several Rab small GTPases, key regulators of membrane trafficking, have recently been reported to participate in ciliogenesis. However, the precise mechanisms of Rab-mediated membrane trafficking during ciliogenesis largely remain unknown. In this thesis, I used a collection of siRNAs against 62 human Rabs to perform a comprehensive knockdown screening for Rabs that regulate serum-starvation-induced ciliogenesis in human telomerase reverse transcriptase retinal pigment epithelium 1 (hTERT-RPE1) cells and succeeded in identifying Rab34 as an essential Rab. Knockout (KO) of Rab34, but not of Rabs previously reported to regulate ciliogenesis (e.g., Rab8 and Rab10), in hTERT-RPE1 cells drastically impaired serum-starvation-induced ciliogenesis. Rab34 was also required for serum-starvation-induced ciliogenesis in NIH/3T3 cells and MCF10A cells, but not for ciliogenesis in Madin-Darby canine kidney (MDCK)-II cysts. I then attempted to identify a specific region(s) of Rab34 that is essential for serum-starvation-induced ciliogenesis in hTERT-RPE1 cells by performing deletion and mutation analyses of Rab34. Instead of a specific sequence in the switch II region, which is generally important for recognizing effector proteins (e.g., Rab interacting lysosomal protein [RILP]), a unique long N-terminal region (amino acids 1–49) of Rab34 before the conserved GTPase domain was found to be essential. Moreover, I performed an in-depth deletion analysis of the N-terminal region of Rab34 together with Ala-based site-directed mutagenesis to identify the essential amino acids required for ciliogenesis. The results showed that a Rab34 mutant lacking an N-terminal 18 amino acids and a Rab34 mutant carrying an LPQ-to-AAA mutation (amino acids 16–18) failed to rescue a Rab34-KO phenotype. I also found that Rab36, the closest paralogue of Rab34, which lacks an LPQ sequence in its N-terminal region failed to restore ciliogenesis. These findings suggest that Rab34 is an atypical Rab that regulates serum-starvation-induced ciliogenesis through the Leu-Pro-Gln sequence of Rab34, which is highly conserved in vertebrates.

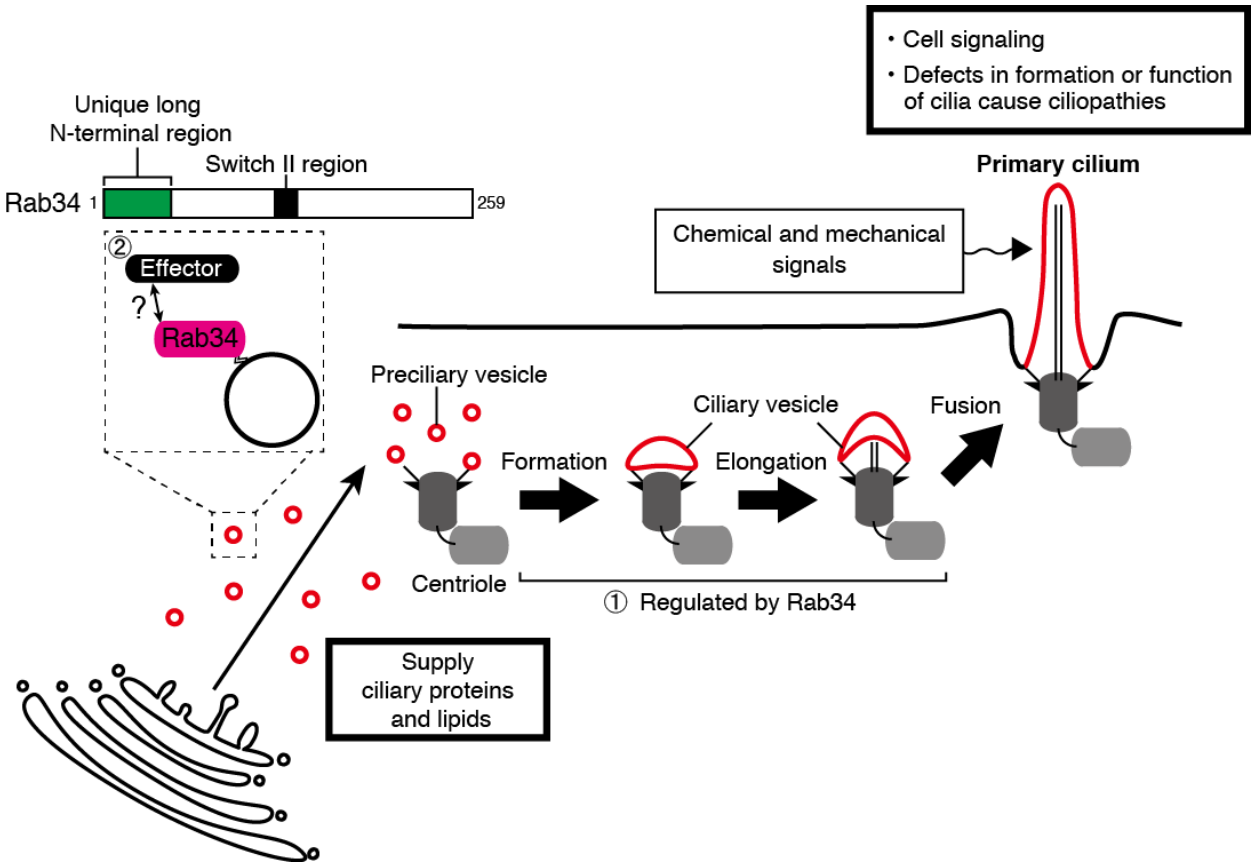

Graphical abstract. Schematic representation of a summary of this thesis

Introduction

Primary cilia are microtubule-based membrane projections from the cell surface and are thought to function as sensors of chemical and mechanical signals in the extracellular environment (Satir and Christensen, 2007). Defects in the formation or function of primary cilia cause various human diseases called ciliopathies (Reiter and Leroux, 2017). The assembly and disassembly of primary cilia are tightly coupled to cell cycle progression, and primary cilia form in cells in the resting stage (Izawa *et al*., 2015). Primary cilium formation (so-called ciliogenesis) is known to occur in a series of membrane trafficking steps (Sánchez and Dynlacht, 2016; Sorokin, 1962; Sorokin, 1968). First, small vesicles called preciliary vesicles accumulate on the mother centriole, and then the preciliary vesicles fuse with each other to form a large vesicle called a ciliary vesicle. The resulting ciliary vesicle extends together with the axoneme, and finally fuses with the plasma membrane (see Graphical abstract). It is generally thought that lipids and ciliary proteins must be transported from other organelles, such as the Golgi apparatus and recycling endosomes, to the mother centriole via membrane trafficking mechanisms during the ciliary vesicle formation and elongation (Follit *et al*., 2006; Knödler *et al*., 2010).

Rab small GTPases, which belong to the Ras superfamily, are key regulators of membrane trafficking (Fukuda, 2008; Stenmark, 2009; Hutagalung and Novick, 2011; Pfeffer, 2013). Rabs function as switch proteins that cycle between an active state and an inactive state. In their active state, Rabs localize to specific vesicles or organelles and recruit a specific binding partner (called a Rab effector) via which they regulate a specific membrane trafficking pathway. Recent studies have reported that several Rabs, including Rab8, Rab10, Rab11, Rab23, Rab29, and Rab34, participate in ciliogenesis (Knödler *et al*., 2010; Yoshimura *et al*., 2007; Nachury *et al*., 2007; Sato *et al*., 2014; Onnis *et al*., 2015; Pusapati *et al*., 2018; Xu *et al*., 2018; Gerondopoulos *et al*., 2019). However, not all of the membrane trafficking mechanisms in ciliogenesis are fully understood, and knockout mice in which each of several cilia-regulating Rabs had been knocked out did not exhibit any ciliopathy phenotypes (Sato *et al*., 2014; Sobajima *et al*., 2014). Moreover, no attempts have been made to perform a comprehensive analysis of all mammalian Rabs (Rab1A–43) during ciliogenesis.

In this thesis, I performed a comprehensive knockdown screening for Rabs that regulate serum-starvation-induced ciliogenesis in human telomerase reverse transcriptase retinal pigment epithelium 1 (hTERT-RPE1) cells and succeeded in identifying Rab34 as an essential Rab in

serum-starvation-induced ciliogenesis. Intriguingly, however, the known cilia-regulating Rabs, including Rab8, Rab10, Rab11B, and Rab12, were found to be dispensable for ciliogenesis, because their knockout (KO) cells formed primary cilia. Moreover, the requirement of Rab34 for serum-starvation-induced ciliogenesis was confirmed in NIH/3T3 cells and MCF10A cells. On the other hand, however, Rab34 was not essential for ciliogenesis in cysts of Madin-Darby canine kidney (MDCK)-II cells. I then performed KO–rescue experiments on several Rab34 mutants, including a switch II swapping mutant (S1A) and an N-terminal 49 amino acids [AA] deletion mutant (ΔN49), to identify the region of Rab34 that is responsible for ciliogenesis. The results suggest that an N-terminal region (AA1–49), but not a switch II region of Rab34 is required for ciliogenesis. I further analyzed the N-terminal region of Rab34 in greater detail by means of Ala-based site-directed mutagenesis and identifed key amino acids that are essential for ciliogenesis in hTERT-RPE1 cells. These findings indicate that the unique long N-terminal region (especially AA16–18) of Rab34, and not a specific sequence in the switch II region, is necessary for serum-starvation-induced ciliogenesis.

Material and Methods

Antibodies

Anti-acetylated tubulin mouse monoclonal antibody (#T7451), anti-γ tubulin mouse monoclonal antibody (#T5326), anti-FLAG tag (M2) mouse monoclonal antibody (#F1804), anti-GALNT2 rabbit polyclonal antibody (#HPA011222), horseradish-peroxidase (HRP)-conjugated anti-T7 tag antibody (#69522), and HRP-conjugated anti-FLAG tag (M2) antibody (#A8592) were obtained from Sigma-Aldrich. Anti-Arl13B rabbit polyclonal antibody (#17711-1-AP), anti-CP110 rabbit polyclonal antibody (#12780-1-AP), anti-IFT20 rabbit polyclonal antibody (#13615-1-AP), and anti-RILP rabbit polyclonal antibody (#13574-1-AP) were from Proteintech. Anti-Rab10 rabbit polyclonal antibody (#8127) and anti-FLCN (Folliculin) rabbit polyclonal antibody (#13697) were obtained form Cell Signaling Technology. Anti-Rab8 mouse monoclonal antibody (#610845, BD Biosciences), anti-β-actin mouse monoclonal antibody (#G043, Applied Biological Materials), and anti-Munc13-2 (UNC13B) rabbit polyclonal antibody (#ab97924, Abcam) were also obtained commercially. HRP-conjugated anti-mouse IgG goat polyclonal antibody (#1031-05) and anti-rabbit IgG goat polyclonal antibody (#NA934) were from SouthernBiotech and GE Healthcare, respectively. Alexa Fluor 488/555/594/633-conjugated anti-mouse/rabbit IgG goat/donkey polyclonal antibodies were from Thermo Fisher Scientific. Anti-Rab11B, anti-Rab12, and anti-Rab34 rabbit polyclonal antibodies were prepared as described previously (Homma *et al*., 2019; Matsui *et al*., 2011).

siRNAs and plasmids

The sequences of the effective siRNAs against human Rabs are described in previous study (Aizawa and Fukuda, 2015) (Table 1). The nomenclature of human Rabs is in accordance with the National Center for Biotechnology Information (NCBI) database rather than Itoh *et al*., 2006, and thus four Rabs, i.e., Rab7B(42), Rab41(6D), Rab42(43), and Rab43(41), are named in this study as shown before parenthesis, and in previous studies as shown in each parenthesis. The siRNAs against human CEP164, RILP, FLCN (#1 and #2), and Munc13-2 were chemically synthesized by Nippon Gene (Toyama, Japan) (their target sequence is summarized in Table 1). The siRNA-resistant (SR) form of human Rab34 (Aizawa and Fukuda, 2015), Rab34^{SR}(K115A/C116A), Rab34(S1A), Rab34(ΔN49) (deletion of the N-terminal 49 amino acids), Rab34(ΔN18) (deletion of the N-terminal 18 amino acids),

Rab34(ΔN6) (deletion of the N-terminal 6 amino acids), Rab34(A1) (VRR [Val-Arg-Arg]-to-AAA [Ala-Ala-Ala] mutation), Rab34(A2) (DRV [Asp-Arg-Val]-to-AAA mutation), Rab34(A3) (LAE [Leu-Ala-Glu]-to-AAA mutation), Rab34(A4) (LPQ [Leu-Pro-Gln]-to-AAA mutation), Rab34(LA) (Leu-to-Ala mutation), Rab34(PA) (Pro-to-Ala mutaion), and Rab34(QA) (Gln-to-Ala mutation) were prepared by conventional PCR techniques using the specific oligonucleotides shown in Table 1 as described previously (Fukuda *et al*., 1995) and subcloned into the pMRX-IRES-puro-EGFP, pMRX-IRES-bsr-EGFP-P2A, pEF-FLAG tag (Fukuda *et al*., 1999), and pGBD-C1 vectors (James *et al*., 1996). The cDNAs of mouse Rab34 (Fukuda *et al*., 2002), Rab34(T66N), and Rab34(Q111L) (Ishida *et al*., 2012) were subcloned into the pMRX-IRES-bsr-EGFP-P2A vector and pMRX-IRES-bsr vector, respectively. The P2A self-cleavage site (ATNFSLLKQAGDVEENPGP; [Kim *et al*., 2011]) was inserted into the pMRX-IRES-bsr-EGFP vector by PCR using specific oligonucleotides (Table 1). The pMRX-IRES-puro/bsr-EGFP vectors are variants of the pMRX-IRES-puro/bsr vectors, which were donated by Dr. Shoji Yamaoka (Tokyo Medical and Dental University, Tokyo, Japan). pEF-FLAG-Rab34 and pEF-T7-RILP were prepared as described previously (Matsui *et al*., 2012; Fukuda *et al*., 2002). The cDNAs of mouse RILP-L1 and RILP-L2 (Matsui *et al*., 2012) were subcloned into the pAct2 vector (Clontech/Takara Bio, Shiga, Japan).

The target sequences for human Rab8A/B-KO, Rab10-KO, Rab11B-KO, Rab12-KO, and Rab34-KO were designed by using CRISPR direct (https://crispr.dbcls.jp/) (summarized in Table 1). The annealed oligonucleotides of the Rab8A/B-KO and Rab11B-KO sense and antisense oligonucleotides were inserted into the pSpCas9(BB)-2A-bsr vector, a variant of pSpCas9(BB)-2A-puro (ID# 48139) that was obtained by replacement of the puromycin S-resistant gene (puro) by a blasticidin-resistant gene (bsr). The annealed oligonucleotides for Rab10-KO, Rab12-KO, and Rab34-KO were also inserted into the pSpCas9(BB)-2A-puro vector and pDonor-tBFP-NLS-Neo vector (Addgene ID# 80766).

Cell culture and transfections

hTERT-RPE1 cells were cultured at 37ºC under 5% CO_2 in Dulbecco's Modified Eagle Medium: Nutrient Mixture F-12 (DMEM/F12) medium (Thermo Fisher Scientific) supplemented with 10% fetal bovine serum, 100 μg/mL streptomycin, and 100 unit/mL penicillin G. One day after plating, siRNAs and plasmids were transfected into hTERT-RPE1 cells by using Lipofectamine RNAi MAX for

the siRNAs (concentrations are indicated in each figure legend) and Lipofectamine 2000 (Thermo Fisher Scientific) or Fugene6 (Promega) for the plasmids each according to the manufacturer's instructions.

MCF10A cells were cultured at 37ºC under 5% CO_2 in DMEM/F12 medium supplemented with 5% horse serum, 50 ng/mL cholera toxin (Fujifilm Wako Pure Chemical, Osaka, Japan), 20 ng/mL epidermal growth factor (Fujifilm Wako Pure Chemical), 10 μg/mL insulin (Fujifilm Wako Pure Chemical), 500 ng/mL hydrocortisone (Fujifilm Wako Pure Chemical), 100 μg/mL streptomycin, and 100 unit/mL penicillin G. One day after plating, siRNAs (0.5 nM) were transfected into MCF10A cells by using Lipofectamine RNAiMAX according to the manufacturer's instructions. The same culture medium without the addition of horse serum and cholera toxin was used for serum starvation.

MDCK-II cells and NIH/3T3 cells were cultured at 37ºC under 5% CO_2 in DMEM medium supplemented with 10% fetal bovine serum, 100 μg/mL streptomycin, and 100 unit/mL penicillin G. Establishment of Rab-KO MDCK-II cells (listed in Fig. 7) was performed as described previously (Homma *et al*., 2019). For culture of three-dimensional cysts, MDCK-II cells were suspended in culture medium containing 10mM HEPES and 2 mg/mL collagen. This mixture was placed in a 24-well plate, added with 1.6 mL of the culture medium and cultured for 7-day. Plat-E cells were donated by Dr. Toshio Kitamura (The University of Tokyo, Tokyo, Japan). The plat-E cell culture and retrovirus infection were performed as described previously (Morita *et al*., 2000).

Establishment of CRISPR/Cas9 KO cell lines

hTERT-RPE1 cells that had been transfected with pSpCas9-bsr-Rab8A/B or -Rab11B were selected by exposure to 15 μg/mL blasticidin S for ~48 h. hTERT-RPE1 cells that had been transfected with pSpCas9-puro-Rab10, -Rab12, or -Rab34 and pDonor-tBFP-NLS-Neo-Rab10, -Rab12 or -Rab34 were selected as described previously (Katoh *et al*., 2017). Single clones were then selected by the limiting dilution method. KO cells were first checked for loss of target proteins by immunoblotting, and then checked for genomic mutations by genomic PCR and sequencing of the PCR products as described previously (Homma *et al*., 2019). Rab34-KO NIH/3T3 cells were established in a similar manner.

Immunoblotting

hTERT-RPE1 cells were lysed in an SDS sample buffer (62.5 mM Tris-HCl, pH6.8, 2%

2-mercaptoehanol, 10% glycerol, and 0.02% Bromophenol blue) in a lysis buffer (50 mM HEPES-KOH, pH7.2, 150 mM NaCl, 1 mM $MgCl_2$, and 1% Triton X-100). Cell lysates were subjected to 5%, 10%, or 12.5% SDS-PAGE, and proteins were transferred to PVDF membranes (Merck Millipore). The membranes were blocked with 1% or 5% skim milk and 0.1% Tween-20 in PBS and then reacted with specific primary antibodies. The reacted bands were visualized with appropriate HRP-conjugated secondary antibodies and detected by enhanced chemiluminescence.

Immunofluorescence analysis

hTERT-RPE1 cells, NIH/3T3 cells, and MCF10A cells that had been transfected with siRNAs or in which a *Rab* had been knocked out were fixed with 4% paraformaldehyde for 15 min at room temperature after 24-h or 48-h serum starvation. After fixation, the cells were permeabilized with 0.3% Triton X-100 in PBS for 1 min and then stained with specific primary antibodies and appropriate Alexa Fluor 488/555/633-conjugated secondary antibodies. After 7-day culture in collagen gel MDCK-II cysts were fixed with 10% trichloroacetic acid (TCA) for 15 min at room temperature and then stained with specific primary antibodies and appropriate Alexa Fluor 555/633-conjugated secondary antibodies. The immunostained cells were examined with a confocal fluorescence microscope (FV1000, FV1000-D; Olympus, Tokyo, Japan; and Dragonfly spinning disk scanning unit (Dragonfly200); Andor, Belfast, Northern Ireland).

Binding experiments

Yeast two-hybrid assays were performed by using pGBD-C1-Rab34(WT), -Rab34(KC/AA), Rab34(S1A), or -Rab34(ΔN49) and pAct2-RILP as described previously (Tamura *et al*., 2009). The yeast strain, medium, culture conditions, and transformation protocol were as described previously (James et al., 1996).

FLAG-tagged Rab34(WT), Rab34(KC/AA), or Rab34(S1A) and T7-tagged GFP or RILP were co-expressed in COS7 cells, and their interaction was analyzed by co-immunoprecipitation. COS7 cell lysates were incubated with anti-T7-tag-antibody-conjugated agarose beads. Proteins bound to the beads and a 1 % volume of total cell lysates were analyzed by immunoblotting with HRP-conjugated anti-FLAG and anti-T7 tag antibodies as described previously (Fukuda *et al*., 1999; Kobayashi *et al*.,

2015).

Statistical analysis

The data were statistically analyzed by performing Student's unpaired *t*-test, Dunnett's test, or the Tukey-Kramer test. The single asterisk (*), double asterisks (**), and triple asterisks (***) in the graphs indicate p values <0.05, <0.01, and <0.001, respectively. NS indicates not significant (p value >0.05).

Results

Comprehensive screening for Rabs whose knockdown inhibits ciliogenesis in hTERT-RPE1 cells

To identify novel Rabs that participate in serum-starvation-induced primary ciliogenesis, by using effective and specific siRNAs against 62 human Rabs that have developed previously in our laboratory (Aizawa and Fukuda, 2015), I performed a comprehensive knockdown screening in hTERT-RPE1 cells. I used acetylated tubulin as a cilium marker and then counted the percentage of non-ciliated cells. When I knocked down CEP164 protein that is essential for ciliogenesis (Graser *et al*., 2007), the percentage of non-ciliated cells increased to more than 80% (Fig. 1*A*, *black bar*), whereas control siRNA had almost no effect (~10% of the cells were non-ciliated), thereby validating this experimental setup. The results of the screening showed that knockdown of ten Rabs, i.e., Rab6C, Rab9A, Rab10, Rab11B, Rab12, Rab34, Rab40A, Rab40B, Rab42(43), and Rab43(41), increased the percentage of non-ciliated cells to more than 50% (Fig. 1*A* blue bars, and 1*B*), and I considered these Rabs to be primary candidates.

To confirm the knockdown effects on ciliogenesis that had been observed in the first screening and to avoid possible off-target effects by single siRNAs, I proceeded to perform knockdown experiments by using other independent siRNAs against the primary Rab candidates. The results showed that knockdown of only four Rabs, i.e., Rab6C, Rab11B, Rab12, and Rab34, by each of two independent siRNAs increased the percentage of non-ciliated cells to more than 50% (Fig. 2*A*). I also checked the protein expression levels of several candidate Rabs by immunoblotting, and the results confirmed that the Rab11B, Rab12, and Rab34 bands almost completely disappeared when the two independent siRNAs were used (Fig. 2*B*). siRab9A#2 and siRab10#2 seemed to decrease the protein expression level more efficiently than siRab9A#1 and siRab10#1, respectively, did (Fig. 2*B* and data not shown), but they had a lesser effect on ciliogenesis, suggesting that siRab9A#1 and siRab10#1 have certain off-target effects on ciliogenesis. On the other hand, no protein expression of other candidate Rabs, including Rab6C, was detected by immunoblotting (data not shown), and I did not pursue Rab6C in the subsequent analysis. Based on the results of the two-step screenings, I selected Rab11B, Rab12, and Rab34 as secondary candidate Rabs.

A possible function of Rab11 in ciliogenesis had already been reported (Knödler *et al*., 2010),

but involvement of Rab12 and Rab34 in ciliogenesis had not been investigated by the time I completed the comprehensive screening. During the course of investigating Rab12 and Rab34 in the subsequent analysis, their possible involvement in ciliogenesis was reported by other groups (Pusapati *et al*., 2018, Steger *et al*., 2017; Xu *et al*., 2018; Breslow *et al*., 2018), although the detailed molecular mechanisms remained unknown.

Rab34 is required for ciliogenesis in hTERT-RPE1 cells

To determine whether the secondary candidates identified above, i.e., Rab11B, Rab12, and Rab34, are indeed essential for ciliogenesis in hTERT-RPE1 cells, I generated their respective KO cells by using the CRISPR/Cas9 system. I also established Rab8A/B-double KO (Rab8A/B-KO) cells and Rab8A/B/10-triple KO (Rab8A/B/10-KO) cells as controls, because Rab8 and Rab10 are widely thought to be involved in cilium formation in mammalian cultured cells (Sato e*t al*., 2014). Loss of the target Rabs in each KO cell was verified by both immunoblotting (Fig. 3*B*) and sequencing of genomic PCR products (Fig. 4). As shown in Fig. 3*A*, only Rab34-KO greatly increased the percentage of non-ciliated cells. By contrast, Rab8A/B-KO, Rab10-KO, Rab8A/B/10-KO, Rab11B-KO, and Rab12-KO cells did not show any defects in ciliogenesis under my experimental conditions. The KO phenotypes observed in this study are unlikely to be caused by clonal variations, because essentially the same results were obtained in other independent Rab-KO clones (i.e., impaired ciliogenesis in Rab34-KO cells versus normal ciliogenesis in other Rab-KO cells) (data not shown).

To further confirm that the impaired ciliogenesis was directly related to Rab34-KO, I performed rescue experiments by stably expressing EGFP (enhanced green fluorescent protein)-P2A-Rab34, which contains a P2A self-cleavage site (Kim *et al*., 2011) between EGFP and Rab34, in Rab34-KO cells (Fig. 5*A*). The results showed that expression of EGFP-P2A-Rab34 completely rescued the impaired ciliogenesis phenotype of Rab34-KO cells (Fig. 3*C* and 3*D*). I used EGFP-P2A-Rab34 instead of EGFP-Rab34 for the KO–rescue experiment, because EGFP-P2A-Rab34 was able to rescue the phenotype of Rab34-knockdown (KD) cells more efficiently than EGFP-Rab34 was (Fig. 5*B*), suggesting that N-terminal EGFP-tagging partly distorts the function of Rab34. A similar observation was previously reported with respect to Rab10: untagged Rab10, but not EGFP-Rab10, was found to promote neurite outgrowth of Rab10-depleted cells (Homma and Fukuda, 2016). These

findings suggest that Rab34 is the most crucial Rab for serum-starvation-induced ciliogenesis in hTERT-RPE1 cells.

Requirement of Rab34 for ciliogenesis depends on the cell type

To determine whether Rab34 is a general positive regulator of ciliogenesis, I investigated the effect of Rab34-KO or -KD on ciliogenesis in other cell types. As shown in Fig. 6*A* and 6*B*, Rab34 depletion in NIH/3T3 cells and MCF10A cells resulted in increase in the percentage of non-ciliated cells and decrease in the ciliated cells under serum-starved conditions, respectively, and the impaired ciliogenesis of Rab34-KO NIH/3T3 cells and Rab34-KD MCF10A cells was clearly rescued by expression of EGFP-P2A-Rab34. On the other hand, checking the primary cilia in the cysts of Rab-KO MDCK-II cells that recently established in our laboratory (Homma *et al*., 2019) revealed that all of the Rab-KO cysts, including the Rab34-KO cysts, had formed primary cilia in their luminal domain (Fig. 6*C* and Fig. 7). Although Rab6 and Rab11 have been shown to be required for normal epithelial morphogenesis (Homma *et al*., 2019), their KO cysts still had primary cilia in their luminal domain (Fig. 6*D*). Thus, Rab34 is unlikely to be a general regulator of ciliogenesis, and it is dispensable for ciliogenesis at least in MDCK-II cysts.

Rab34 is required for early steps in serum-starvation-induced ciliogenesis in hTERT-RPE1 cells

To investigate the defective ciliogenesis in the absence of Rab34 in greater detail, I then investigated the subcellular localization of ciliary membrane proteins and proteins that are required for ciliogenesis, i.e., Rabin8, CP110, IFT20, and Arl13B (Follit *et al*., 2006, Nachury *et al*., 2007, Spektor *et al*., 2007, Larkins *et al*., 2011), in Rab34-KO cells. As shown in Fig. 8*A*, Rab34-KO had no effect on the localization of Rabin8 (1 h after serum starvation) or of CP110, IFT20, and Arl13B (24 h after serum starvation) in hTERT-RPE1 cells, when compared with the control parental cells; removal of CP110 from mother centrioles (Fig. 8*A*, *arrows* in the *second panels*) (Spektor *et al*., 2007), and the centriole localization of Rabin8, IFT20, and Arl13B (Fig. 8*A*, *arrowheads* in the *top*, *third*, *and bottom panels*, respectively). Essentially the same results were reported for CP110, Rabin8, and IFT20 in Rab34-KO NIH/3T3 cells (Xu *et al*., 2018), indicating that Rab34 is not involved in the recruitment of Rabin8 and

IFT20 to centrioles or CP110 removal. Since depletion of Rab34 inhibited the axoneme elongation and extension of ciliary vesicles, Rab34 is likely to be required for early steps in serum-starvation-induced ciliogenesis in hTERT-RPE1 cells.

Because anti-Rab34 antibody used in this thesis was unable to detect the subcellular localization of endogenous Rab34 in hTERT-RPE1 cells by the immunofluorescence analysis, I tried overexpressing FLAG-tagged Rab34, which can restore the Rab34-KO phenotype in Rab34-KO cells (Fig. 10*D*), and visualized it by using an anti-FLAG tag antibody. The results showed that FLAG-Rab34 was mainly localized at the Golgi apparatus, consistent with the findings in a previous report (Wang and Hong, 2002), and that it rarely localized at primary cilia (approximately 20 %) (Fig. 8*B*). Taken together, these results imply that Rab34, an early-step regulator of ciliogenesis, is likely to be released from ciliary membranes before the maturation of primary cilia.

The unique long N-terminal region of Rab34 is required for ciliogenesis in hTERT-RPE1 cells

Next, I attempted to identify a specific region(s) of Rab34 that is essential for ciliogenesis by performing mutation and deletion analyses of Rab34-KO cells. In general, Rabs are thought to recognize specific effectors through their switch II region, because mutations of specific amino acids in this region of some Rabs have been shown to abrogate their effector-binding ability (Kloer *et al*., 2010; Tamura *et al*., 2011; Etoh and Fukuda, 2015; Matsui *et al*., 2012; Homma *et al*., 2020). Sequence comparisons of the switch II region of mammalian Rabs have revealed that Lys-115 and Cys-116 are specific to Rab34 (and its closest paralog Rab36) (Matsui *et al*., 2012; Fig. 10*A*, *asterisks*). Actually, our group had previously shown that K120A/C121A mutations of Rab36 impaired RILP (Rab interacting lysosomal protein)-binding activity, and that the Rab36(K120A/C121A) mutant did not support retrograde melanosome transport in melanocytes (Matsui *et al*., 2012). I therefore generated a Rab34(K115A/C116A) (simply referred to as Rab34(KC/AA) hereafter) mutant and evaluated its effect on ciliogenesis in Rab34-KO hTERT-RPE1 cells.

Consistent with the previous finding regarding Rab36 (Matsui *et al*., 2012), Rab34(KC/AA) failed to interact with RILP in yeast two-hybrid assays (Fig. 9*A*) and was shown to hardly interact with it by co-immunoprecipitation assays (Fig. 9*B*). Unexpectedly, however, Rab34(KC/AA) completely

rescued the Rab34-KD phenotype (Fig. 9*C*). Since a weak interaction between Rab34(KC/AA) and RILP was still observed in the co-immunoprecipitation assays (Fig. 9*B*), it was possible that such a weak interaction could rescue the KD phenotype. To rule out this possibility, I generated an additional Rab34 mutant that completely lacks RILP-binding ability by swapping the switch II region of Rab34 for that of Rab1A, a Rab isoform distantly related to Rab34 (named Rab34(S1A)) (Fig. 10*A*), and complete loss of RILP-binding activity by Rab34(S1A) was confirmed by both yeast two-hybrid assays and co-immunoprecipitation assays (Fig. 10*B* and 10*C*). Nevertheless, Rab34(S1A) did rescue the Rab34-KO phenotype, the same as Rab34(WT) did (Fig. 10*D*). Although specific sequence in the switch II region of Rab34 was not essential for ciliogenesis, GTP-binding activity of Rab34 itself was necessary, because a constitutively active Rab34 mutant, Rab34(Q111L), but not its constitutively inactive mutant, Rab34(T66N), completely rescued the Rab34-KD effect on ciliogenesis, the same as Rab34(WT) did (Fig. 11).

To further identify the crucial region of Rab34 for ciliogenesis, I compared the entire sequences of mammalian Rab family members in greater detail and discovered that Rab34 contains a long N-terminal region (*gray box* in Fig. 10*A*) that was not found in other Rab isoforms except Rab36. Rab36, the closest paralog of Rab34, also contains a long N-terminal sequence, but the N-terminal sequences are not well conserved between them. I therefore produced an N-terminal deletion mutant of Rab34 (named Rab34(ΔN49)), which lacks the N-terminal 49 amino acids of Rab34, and performed a rescue experiment. The results showed that Rab34(ΔN49) did not rescue the Rab34-KO phenotype at all (Fig. 10*E*). Although the protein expression level of Rab34(ΔN49) was lower than that of Rab34(WT) and Rab34(S1A), it was higher than that of endogenous Rab34 (Fig. 10*F*). This results suggest that the lack of a rescue effect by Rab34(ΔN49) is unlikely to be attributable to its protein expression level (Fig. 10*F*). Moreover, FLAG-tagged Rab34(S1A) and Rab34(ΔN49) mainly localized at the Golgi apparatus, the same as Rab34(WT) did (Figs. 8*B* and 10*G*). It should be noted that Rab34(S1A) localized at primary cilia to an extent similar to that of Rab34(WT) (approximately 20%), whereas I did not observe any ciliary localization of Rab34(ΔN49) under this experimental conditions. Thus, the unique N-terminal region of Rab34 is not involved in its Golgi localization, but it may be required for its ciliary targeting or localization. However, since the protein expression level of Rab34(ΔN49) was often lower than that of Rab34(WT) and Rab34(S1A) (Figs. 10*F*), I could not

completely rule out the possibility that its low protein expression masked the ciliary localization of Rab34(ΔN49).

The N-terminal Leu-Pro-Gln sequence of Rab34 is involved in ciliogenesis in hTERT-RPE1 cells

To narrow down the region of Rab34 (amino acids [AA]1–49) that is required for ciliogenesis, we first compared the N-terminal regions of the Rab34 of various vertebrate species (Fig. 12*A*) and performed a further deletion analysis. I prepared two additional deletion mutants, named Rab34(ΔN18) (deletion of N-terminal 18AA) and Rab34(ΔN6) (deletion of N-terminal 6AA) (Fig. 12*A*). The results showed that stable expression of Rab34(ΔN6) in Rab34-KO cells significantly restored primary cilium formation, the same as the wild-type Rab34 did, but that Rab34(ΔN18) failed to rescue the Rab34-KO phenotype (Fig. 12*B* and 12*D*). Although the protein expression level of Rab34(ΔN18) was lower than that of Rab34(WT) and Rab34(ΔN6), it was much higher than that of endogenous Rab34 (Fig. 12*C*), thereby excluding the possibility that the lack of a rescue effect was attributable to an insufficient amount of Rab34(ΔN18). Thus, the residues of Rab34 that are crucial for its function in ciliogenesis is likely to lie within AA7–18 of Rab34. To identify the specific residues, we then performed a series of Ala-based site-directed mutagenesis and prepared four additional Rab34 mutants, named Rab34(A1) (triple Ala mutations in AA7–9 [VRR]), Rab34(A2) (triple Ala mutations in AA10–12 [DRV]), Rab34(A3) (triple Ala mutations in AA13–15 [LAE]), and Rab34(A4) (triple Ala mutations in AA16–18 [LPQ]) (Fig. 12*A*). The results of the rescue experiment showed that the Rab34(A1), Rab34(A2), and Rab34(A3) mutants completely rescued the Rab34-KO phenotype, the same as the Rab34(WT) did, whereas the Rab34(A4) mutant failed to completely restore ciligogenesis when compared with Rab34(WT) (Fig. 12*E* and 12*G*). Once again, however, the protein expression level of Rab34(A4) was lower than that of the other Rab34 mutants but higher than that of endogenous Rab34 (Fig. 12*F*). These results suggest that AA16–18 (LPQ) of human (or mouse) Rab34 are important for ciliogenesis in hTERT-RPE1 cells. Moreover, since the protein expression levels of Rab34(ΔN18) and Rab34(A4) were relatively low, Leu-16, Pro-17, and/or Gln-18 may also be required for Rab34 protein stability.

To further evaluate the importance of each AA of the LPQ sequence in ciliogenesis, we prepared three additional Rab34 point mutants carrying a Leu-to-Ala, Pro-to-Ala, and Gln-to-Ala

mutation in the AA positions 16–18, named Rab34(LA), Rab34(PA), and Rab34(QA), respectively. The results of the rescue experiment showed that all three mutants completely rescued the Rab34-KO phenotype like Rab34(WT) did (Fig. 13*A* and 13*C*). Moreover, the protein expression levels of Rab34(LA), Rab34(PA), and Rab34(QA) were almost the same as that of Rab34(WT) did (Fig. 13*B*). These results suggest that a single AA substitution within the LPQ sequence would not impair the ciliary function of Rab34 in cilium formation, and they also suggest that zebrafish Rab34, which contains an LPK sequence (Fig. 12*A*), is capable of mediating ciliogenesis.

Rab36 cannot compensate for the Rab34 function in serum-starvation-induced ciliogenesis

Next, I turned my attention to Rab36, the closest paralog of Rab34 (Homma *et al*., 2020), that also has a unique long N-terminal sequence, which is less homologous to that of Rab34. However, I noted that Pro-22, which is equivalent to the Pro-17 of Rab34, is also found in Rab36 (Fig. 12*A*), and at least one AA substitution in the LPQ sequence of Rab34 did not affect its function in ciliogenesis (Fig. 13). Thus, it was still possible that overexpression of Rab36 might compensate for the function of Rab34 in ciliogenesis of Rab34-KO cells, even though knockdown of Rab36 in hTERT-RPE1 cells was shown no effect on ciliogenesis (Fig. 1*A*). To investigate this possibility, I next overexpressed Rab36 in parental and Rab34-KO hTERT-RPE1 cells, but the results showed that Rab36 did not rescue the Rab34-KO phenotype at all (Fig. 14*A* and 14*C*). Although no endogenous Rab36 protein expression was detected under our experimental conditions, exogenous Rab36 protein was easily detected, suggesting that the lack of a rescue effect by Rab36 was not attributable to its low protein expression level (Fig. 14*B*). These results showed that Rab36 cannot compensate for the function of Rab34 in ciliogenesis, and suggest that two AA substitutions in the LPQ sequence of Rab34 impair its function in ciliogenesis. However, I also found that overexpression of Rab36 itself in parental hTERT-RPE1 cells inhibited ciliogenesis (Fig. 14*A* and 14*C*).

The known Rab34-interacting proteins are not required for ciliogenesis in hTERT-RPE1 cells

In the final set of experiments, I investigated the possible involvement of the known Rab34-intearcting proteins, i.e., RILP, RILP-like 1 (RILP-L1), RILP-like 2 (RILP-L2) (Wang and Hong, 2002; Wang *et al*., 2004, Fukuda *et al*., 2008), Folliculin (FLCN) (Starling *et al*., 2016), and Munc13-2

(Goldenberg and Silverman, 2009), in ciliogenesis in hTERT-RPE1 cells. To narrow down the candidates, I first took advantage of the Rab34(S1A) mutant described above. Because Rab34(S1A) was able to support ciliogenesis (Fig. 10*D*), a Rab34 effector(s) that functions in ciliogenesis was expected to bind to Rab34(S1A). However, RILP and RILP-L1/L2 failed to interact with Rab34(S1A) (Fig. 10*B* and 10*C*; and data not shown), indicating that the RILP-binding activity of Rab34 is not essential for ciliogenesis. Actually, knockdown of endogenous RILP in hTERT-RPE1 cells had no or little effect on ciliogenesis (Fig. 15*A*), and RILP-L1 and RILP-L2 have previously been shown to inhibit rather than promote ciliogenesis in hTERT-RPE1 cells (Schaub and Stearns, 2013). I therefore focused on FLCN, which had previously been shown to be associated with ciliopathy (Luijten *et al*., 2013), and Munc13-2 in subsequent analyses. An immunoblot analysis using specific antibodies showed that FLCN was endogenously expressed in hTERT-RPE1 cells (Fig. 15*B*), but no endogenous Munc13-2 expression was detected under my experimental conditions (Fig. 15*C*). Furthermore, transfection of a specific siRNA for Munc13-2 into hTERT-RPE1 cells had no effect on ciliogenesis (Fig. 15*C*), indicating that Munc13-2 is not a relevant effector in ciliogenesis. Finally, I knocked down endogenous FLCN in hTERT-RPE1 cells, and the results showed that FLCN-KD had no effect on ciliogenesis, even though the FLCN immunoreactive bands almost completely disappeared after treatment with two independent siRNAs (Fig. 15*B*). These findings taken together indicate that the known Rab34-interacting proteins, including RILP and FLCN, are not required for Rab34-regulated serum-starvation-induced ciliogenesis in hTERT-RPE1 cells.

Discussion

In this study, I performed a comprehensive knockdown screening for human Rabs that regulate ciliogenesis (Fig. 1), and based on the results together with the results of KO analyses I succeeded in identifying Rab34 as an essential Rab in serum-starvation-induced ciliogenesis in hTERT-RPE1 cells (Figs. 1–3). Moreover, Rab34-KO had no effect on recruitment of IFT20, Rabin8, and Arl13B to centrioles or removal of CP110 from the mother centriole, but they inhibited axoneme elongation and extension of ciliary vesicles (Fig. 8*A*). These results suggest that Rab34 regulates the ciliary vesicle fusion step and/or the subsequent expansion step of serum-starvation-induced ciliogenesis.

Although ~10 Rabs have been proposed to participate in ciliogenesis in previous studies (Knödler *et al*., 2010; Yoshimura *et al*., 2007; Nachury *et al*., 2007; Sato *et al*., 2014; Onnis *et al*., 2015; Pusapati *et al*., 2018; Dhekne *et al*., 2018; Gerondopoulos *et al*., 2019; Wang *et al*., 2019; Kuhns *et al*., 2019), the results of knockdown or knockout of these Rabs in the present study demonstrated that none of the reported Rabs except Rab34 are essential for serum-starvation-induced ciliogenesis, at least in hTERT-RPE1 cells under my experimental conditions (Figs. 1–3). Among the Rab-KO cells established in this study, only the Rab34-KO cells showed marked inhibition of ciliogenesis, and although Rab8/10-KO seemed to weakly inhibit ciliogenesis, the reduction was not statistically significant (Fig. 3). Nevertheless, I cannot rule out the possibility that Rabs other than Rab34 participate in ciliogenesis in other cell types or under different conditions (e.g., different upstream signals).

Intriguingly, when I checked the primary cilia in the cysts of recently established Rab-KO MDCK-II cells (Homma *et al*., 2019), I found that all of the Rab-KO cysts, including the Rab34-KO cysts, formed primary cilia in their luminal domain (Fig. 6*C* and 6*D*, and Fig. 7). Thus, the mechanism of ciliogenesis in the two cell types is likely to be different. Actually, it has been proposed that ciliogenesis in polarized cells and in non-polarized cells occurs in different pathways (Rohatgi and Snell, 2010; Benmerah, 2013). For example, the cilia in hTERT-RPE1 cells, NIH/3T3 cells, and MCF10A cells are induced by serum starvation, whereas the cilia in MDCK-II cells are induced during cyst growth in the absence of starvation. Thus, the upstream signals of ciliogenesis in hTERT-RPE1 and MDCK-II cells must be different, and Rab34 is specifically required for ciliogenesis in only certain cell types, such as hTERT-RPE1 cells, NIH/3T3 cells, and MCF10A cells. Consistent with this conclusion, Rab34-KO mice exhibited polydactyly, cleft lip, and cleft palate, but they did not have a polycystic kidney disease

phenotype (Dickinson *et al*., 2016; Xu *et al*., 2018), indicating that the primary cilia in their kidney cells are functionally normal.

Several questions regarding the function of Rab34 remain unanswered in this study. First important question that must be answered in a future study concerns the function of the LPQ sequence in unique long N-terminal region of Rab34. Since specific sequence in the switch II region of Rab34 is not essential for serum-starvation-induced ciliogenesis (Fig. 9 and Fig. 10), I hypothesized that the long N-terminal region contributes to recognition of an unidentified Rab34 effector that functions in ciliogenesis. Actually, the N-terminal region of certain Rabs is known to contribute to the effector recognition; e.g., the Tyr-6 in the N-terminal region of Rab27A is required for its interaction with Slac2-a (Kukimoto-Niino *et al.*, 2008) (see Graphical abstract ②). Alternatively, the three amino acids may be involved in an interaction with a certain chaperone (e.g., the Rab10 chaperone RABIF/MSS4 (Gulbranson *et al.*, 2017)) and thereby stabilize Rab34 protein in cells. Consistent with my hypothesis, N-terminal EGFP-tagging of Rab34 significantly reduced its rescue efficiency (Fig. 5), presumably because fusion of a relatively large molecule, e.g., EGFP, to the N-terminus of Rab34 partially impairs its interaction with an unidentified Rab34 effector. In our laboratory N-terminally GST (glutathione *S*-transferase)-tagged or GBD (Gal4-binding domain)-tagged Rab34 were used as bait in previous comprehensive screening for Rab effectors (Matsui *et al*., 2012, Fukuda *et al*., 2008, Kanno *et al*., 2010), but this screening methods are presumably inappropriate for identifying a Rab34 effector that functions in ciliogenesis. C-terminally tagged or untagged Rab34(S1A), which lacks binding activity toward RILP family members, would be useful in future screening for a novel Rab34 effector(s) in ciliogenesis. Second unanswered question concerns the cargo(s) Rab34 transports. One possible cargo is a component of SNARE complexes, because recruitment of an EHD1-binding protein, SNAP-29, to preciliary membranes is important for ciliogenesis, and a similar early step-ciliogenesis-defect phenotype has been observed in EHD1-depleted cells (Lu *et al*., 2015). It is also unknown which membrane trafficking steps(s), e.g., budding, transport, docking, and fusion, Rab34 regulates. It had previously been shown that the main localization of Rab34 is the Golgi apparatus (Wang and Hong, 2002), and I confirmed its Golgi localization in the present study (Fig. 8*B*). The unique N-terminal region (AA1–49) of Rab34 is not required for its Golgi localization, but no ciliary localization of Rab34(ΔN49) was observed at least under my experimental conditions. I therefore assume that Rab34 regulates the budding/secretion step from the Golgi, the transport step of

preciliary vesicles, and/or the fusion step of preciliary vesicles to form ciliary vesicles (see Graphical abstract ①). Third question is why Rab36 has a dominant negative effect on ciliogenesis. We think that there are several possible explanations. Since both Rab34 and Rab36 localize at the perinuclear region (presumably at the Golgi) (Wang and Hong, 2002; Chen *et al.*, 2010), one possible explanation is that exogenous Rab36 affects transport of Golgi-derived vesicles, which are normally transported to preciliary structures (or cilia) via Rab34. Another possible explanation is that Rab36 traps Rab34 effector(s) that is essential for ciliogenesis to indirectly inhibit the function of endogenous Rab34. Actually, the switch II region of Rab34 and Rab36 are highly conserved and they share several effectors such as RILP family members (Chen *et al.*, 2010; Matsui *et al.*, 2012). However, trapping of Rab34 effectors by Rab36 may be unlikely because the RILP family members were showed not to be involved in ciliogenesis in hTERT-RPE1 cells (Fig. 15). In any case, Rab36 could be used as a dominant negative tool to inhibit ciliogenesis in future studies, even though its inhibitory mechanism remains unknown.

In summary, I found that Rab34 regulates early steps of serum-starvation-induced ciliogenesis through its unique, previously uncharacterized N-terminal region (especially AA16–18 (LPQ)) and that its KO causes a loss of primary cilia even after serum starvation. In the future, it will be necessary to identify all of the membrane trafficking mechanisms responsible for Rab34-dependent ciliogenesis and determine the functional relationships between Rab34 and the previously reported Rabs, including Rab8 and Rab11, during ciliogenesis.

References

Aizawa, M., and Fukuda, M. (2015) Small GTPase Rab2B and its specific binding protein Golgi-associated Rab2B interactor-like 4 (GARI-L4) regulate Golgi morphology. *J. Biol. Chem.* **290,** 22250–22261

Benmerah, A. (2013) The ciliary pocket. *Curr. Opin. Cell Biol.* **25,** 78–84

Breslow, D. K., Hoogendoorn, S., Kopp, A. R., Morgens, D. W., Vu, B. K., Kennedy, M. C., Han, K., Li, A., Hess, G. T., Bassik, M. C., Chen, J. K., and Nachury, M. V (2018) A CRISPR-based screen for Headgehog signaling provides insights into ciliary function and ciliopathies. *Nat. Genet.* **50,** 460–471

Chen, L., Hu, J., Yun, Y., and Wang, T. (2010) Rab36 regulates the spatial distribution of late endosomes and lysosomes through a similar mechanism to Rab34. *Mol. Mem. Biol.* **27,** 23-30

Dhekne, H. S., Yanatori, I., Gomewz, R. C., Tonelli, F., Diez, F., Schüle, B., Steger, M., Alessi, D. R., and Pfeffer, S. R. (2018) A pathway for parkinson's disease LRRK2 kinase to block primary cilia and sonic hedgehog signaling in the brain. *eLife* **7,** e40202

Dickinson, M. E., *et al.* (2016) High-throughput discovery of novel developmental phenotypes. *Nature* **537,** 508–514

Etoh, K., and Fukuda, M. (2015) Structure-function analyses of the small GTPase Rab35 and its efffector protein centaurin-β2/ACAP2 during neurite outgrowth of PC12 cells. *J. Biol. Chem.* **290,** 9064–9074

Follit, J. A., Tuft, R. A., Fogarty, K. E., and Pazour, G. J. (2006) The intraflagellar transport protein IFT20 is associated with the Golgi complex and is required for cilia assembly. *Mol. Biol. Cell* **17,** 3781–3792

Fukuda, M. (2008) Regulation of secretory vesicle traffic by Rab small GTPases. *Cell. Mol. Life Sci.* **65,** 2801–2813

Fukuda, M., Kojima, T., Aruga, J., Niinobe, M., and Mikoshiba, K. (1995) Functional diversity of C2 domains of synaptotagmin family: Mutational analysis of inositol high polyphosphate binding domain. *J. Biol. Chem.* **270,** 26523–26527

Fukuda, M., Kanno, E., and Mikoshiba, K. (1999) Conserved N-terminal cysteine motif is essential for homo- and heterodimer formation of synaptotagmins III, V, VI, and X. *J. Biol. Chem.* **274,** 31421–31427

Fukuda, M., Kuroda, T. S., and Mikoshiba, K. (2002) Slac2-a/melanophilin, the missing link between

Rab27 and myosin Va: Implications of a tripartite protein complex for melanosome transport. *J. Biol. Chem.* **277,** 12432–12436

Fukuda, M., Kanno, E., Ishibashi, K., and Itoh, T. (2008) Large scale screening for novel Rab effectors reveals unexpected broad Rab binding specificity. *Mol. Cell. Proteomics* **7,** 1031–1042

Gerondopoulos, A., Strutt, H., Stevenson, N. L., Sobajima, T., Levine, T. P., Stephens, D. J., Strutt, D., and Barr, F. A. (2019) Planar cell polarity effector proteins Inturned and Fuzzy form a Rab23 GEF complex. *Curr. Biol.* **29,** 3323–3330

Goldenberg, N. M., and Silverman, M. (2009) Rab34 and its effector munc13-2 constitute a new pathway modulating protein secretion in the cellular response to hyperglycemia. *Am. J. Physiol. Cell Physiol.* **297,** C1053–C1058

Graser, S., Stierhof, Y. D., Lavoie, S. B., Gassner, O. S., Lamla, S., Le Clech, M., and Nigg, E. A. (2007) Cep164, a novel centriole appendage protein required for primary cilium formation. *J. Cell Biol.* **179,** 321–330

Gulbranson, D. R., Kavis, E. M., Demmitt, B. A., Ouyang, Y., Ye, Y., Yu, H., and Shen, J. (2017) RABIF/MSS4 is a Rab-stabilizing holdase chaperone required for GLUT4 exocytosis. *Proc. Natl. Acad. Sci. U. S. A.* **114,** E8224-E8233

Homma, Y., and Fukuda, M. (2016) Rabin8 regulates neurite outgrowth in both GEF-activity-dependent and -independent manners. *Mol. Biol. Cell* **27,** 2107–2118

Homma, Y., Kinoshita, R., Kuchitsu, Y., Wawro, P. S., Marubashi, S., Oguchi, M. E., Ishida, M., Fujita, N., and Fukuda, M. (2019) Comprehensive knockout analysis of the Rab family GTPases in epithelial cells. *J. Cell Biol.* **218,** 2035–2050

Homma, Y. Hiragi, S., and Fukuda, M. (2020) Rab family of small GTPases: an updated view on their regulation and functions. *FEBS J.* doi: 10.1111/febs.15453

Hutagalung, A. H., and Novick, P. J. (2011) Role of Rab GTPases in membrane traffic and cell physiology. *Physiol. Rev.* **91,** 119–149

Ishida, M., Ohbayashi, N., Maruta, Y., Ebata, Y., and Fukuda, M. (2012) Functional involvement of Rab1A in microtubule-dependent anterograde melanosome transport in melanocytes. *J. Cell Sci.* **125,** 5177–5187

Itoh, T., Satoh, M., Kanno, E., and Fukuda, M. (2006) Screening for target Rabs of TBC

(Tre-2/Bub2/Cdc16) domain-containing proteins based on their Rab-binding activity. *Genes Cells* **11,** 1023–1037

Izawa, I., Goto, H., Kasahara, K., and Inagaki, M. (2015) Current topics of functional links between primary cilia and cell cycle. *Cilia* **4,** 12

James, P., Halladay, J., and Craig, E. A. (1996) Genomic libraries and a host strain designed for highly efficient two-hybrid selection in yeast. *Genetics* **144,** 1425–1436

Kanno, E., Ishibashi, K., Kobayashi, H., Matsui, T., Ohbayashi, N., and Fukuda, M. (2010) Comprehensive screening for novel Rab-binding proteins by GST pull-down assay using 60 different mammalian Rabs. *Traffic* **11,** 491–507

Katoh, Y., Michisaka, S., Nozaki, S., Funabashi, T., Hirano, T., Takei, R., and Nakayama, K. (2017) Practical method for targeted disruption of cilia-related genes by using CRISPR/Cas9-mediated, homology-independent knock-in system. *Mol. Biol. Cell* **28,** 898–906

Kim, J. H., Lee, S. R., Li, L. H., Park, H. J., Park, J. H., Lee, K. Y., Kim, M. K., Shin, B. A., and Choi, S. Y. (2011) High cleavage efficiency of a 2A peptide derived from porcine teschovirus-1 in human cell lines, zebrafish and mice. *PLoS One*. **6,** e18556

Kloer, D. P., Rojas, R., Ivan, V., Moriyama, K., van Vlijmen, T., Murthy, N., Ghirlando, R., van der Sluijs, P., Hurley, J. H., and Bonifacino, J. S. (2010) Assembly of the biogenesis of lysosome-related organelles complex-3 (BLOC-3) and its interaction with Rab9. *J. Biol. Chem*. **285,** 7794–7804

Knödler, A., Feng, S., Zhang, J., Zhang, X., Das, A., Peränen, J., and Guo, W. (2010) Coordination of Rab8 and Rab11 in primary ciliogenesis. *Proc. Natl. Acad. Sci. U. S. A*. **107,** 6346–6351

Kobayashi, H., Etoh, K., Marubashi, S., Ohbayashi, N., and Fukuda, M. (2015) Measurement of Rab35 activity with the GTP-Rab35 trapper RBD35. *Methods Mol. Biol*. **1298,** 207–216

Kuhns, S., Seixas, C., Pestana, S., Tavares, B., Nogueira, R., Jacinto, R., Ramalho, J. S., Simpson, J. C., Andersen, J. S., Echard, A., Lopes, S. S., Barral, D. C., and Blacque, O. E. (2019) Rab35 controls cilium length, function and membrane composition. *EMBO Rep*. **20,** e47625

Kukimoto-Niino, M., Sakamoto, A., Kanno, E., Hanawa-Suetsugu, K., Terada, T., Shirouzu, M., Fukuda, M., and Yokoyama. S. (2008) Structural basis for the exclusive specificity of Slac2-a/melanophilin for the Rab27 GTPases. *Structure* **16,** 1478-1490

Larkins, C. E., Aviles, G. D. G., East, M. P., Kahn, R. A., and Caspary, T. (2011) Arl13b regulates

ciliogenesis and the dynamic localization of Shh signaling proteins. *Mol. Biol. Cell* **22,** 4694–4703

Lu, Q., Insinna, C., Ott, C., Stauffer, J., Pintado, P. A., Rahajeng, J., Baxa, U., Walia, V., Cuenca, A., Hwang, Y.-S., Daar, I. O., Lopes, S., Lippincott-Schwartz, J., Jackson, P. K., Caplan, S., and Westlake, C. J. (2015) Early steps in primary cilium assembly require EHD1/EHD3-dependent ciliary vesicle formation. *Nat. Cell Biol.* **17,** 228–240

Luijten, M. N. H., Basten, S. G., Claessens, T., Vernooij, M., Scott, C. L., Janssen, R., Easton, J. A., Kamps, M. A. F., Vreeburg, M., Broers, J. L. V., van Geel, M., Menko, F. H., Harbottle, R. P., Nookala, R. K., Tee, A. R., Land, S. C., Giles, R. H., Coull, B. J., and van Steensel, M. A. M. (2013) Birt-Hogg-Dube syndrome is a novel ciliopathy. *Hum. Mol. Genet.* **22,** 4383–4397

Matsui, T., and Fukuda, M. (2013) Rab12 regulates mTORC1 activity and autophagy through controlling the degradation of amino-acid transporter PAT4. *EMBO Rep.* **14,** 450–457

Matsui, T., Itoh, T., and Fukuda, M. (2011) Small GTPase Rab12 regulates constitutive degradation of transferrin receptor. *Traffic* **12,** 1432–1443

Matsui, T., Ohbayashi, N., and Fukuda, M. (2012) The Rab interacting lysosomal protein (RILP) homology domain functions as a novel effector domain for small GTPase Rab36: Rab36 regulates retrograde melanosome transport in melanocytes. *J. Biol. Chem.* **287,** 28619–28631

Morita, S., Kojima, T., and Kitamura, T. (2000). Plat-E: An efficient and stable system for transient packaging of retroviruses. *Gene Ther.* **7,** 1063–1066

Nachury, M. V., Loktev, A. V., Zhang, Q., Westlake, C. J., Peränen, J., Merdes, A., Slusarski, D. C., Scheller, R. H., Bazan, J. F., Sheffield, V. C., and Jackson, P. K. (2007) A core complex of BBS proteins cooperates with the GTPase Rab8 to promote ciliary membrane biogenesis. *Cell* **129,** 1201–1213

Onnis, A., Finetti, F., Patrussi, L., Gottardo, M., Cassioli, C., Spanò, S., and Baldari, C. T. (2015) The small GTPase Rab29 is a common regulator of immune synapse assembly and ciliogenesis. *Cell Death Differ.* **22,** 1687–1699

Pfeffer, S. R. (2013) Rab GTPase regulation of membrane identity. *Curr. Opin. Cell Biol.* **25,** 414–419

Pusapati, G. V., Kong, J. H., Patel, B. B., Krishnan, A., Sagner, A., Kinnebrew, M., Briscoe, J., Aravind, L., and Rohatgi, R. (2018) CRISPR screens uncover genes that regulate target cell sensitivity to the morphogen sonic hedgehog. *Dev. Cell* **44,** 113–129

Reiter, J. F., and Leroux, M. R. (2017) Genes and molecular pathways underpinning ciliopathies. *Nat. Rev. Mol. Cell Biol.* **18,** 533–547

Rohatgi, R., and Snell, W. J. (2010) The ciliary membrane. *Curr. Opin. Cell Biol.* **22,** 541–546

Sánchez, I., and Dynlacht, B. D. (2016) Cilium assembly and disassembly. *Nat. Cell Biol.* **18,** 711–717

Satir, P., and Christensen, S. T. (2007) Overview of structure and function of mammalian cilia. *Annu. Rev. Physiol.* **69,** 377–400

Sato, T., Iwano, T., Kunii, M., Matsuda, S., Mizuguchi, R., Jung, Y., Hagiwara, H., Yoshihara, Y., Yuzaki, M., Harada, R., and Harada, A. (2014) Rab8a and Rab8b are essential for several apical transport pathways but insufficient for ciliogenesis. *J. Cell Sci.* **127,** 422–431

Schaub, J. R., and Stearns, T. (2013) The Rilp-like proteins Rilpl1 and Rilpl2 regulate ciliary membrane content. *Mol. Biol. Cell* **24,** 453–464

Sorokin, S. (1962) Centrioles rudimentary and smooth and the formation of cilia muscle by fibroblasts. *J. Cell Biol.* **15,** 363–377

Sorokin, S. P. (1968) Reconstructions of centriole formation and ciliogenesis in mammalian lungs. *J. Cell Sci.* **3,** 207–230

Sobajima, T., Yoshimura, S., Iwano, T., Kunii, M., Watanabe, M., Atik, N., Mushiake, S., Morii, E., Koyama, Y., Miyoshi, E., and Harada, A. (2014) Rab11a is required for apical protein localisation in the intestine. *Biol. Open* **4,** 86–94

Spektor, A., Tsang, W. Y., Khoo, D., and Dynlacht, B. D. (2007) Cep97 and CP110 suppress a cilia assembly program. *Cell* **130,** 678–690

Starling, G. P., Yip, Y. Y., Sanger, A., Morton, P. E., Eden, E. R., and Dodding, M. P. (2016) Folliculin directs the formation of a Rab34-RILP complex to control the nutrient-dependent dynamic distribution of lysosomes. *EMBO Rep.* **17,** 823–841

Steger, M., Diez, F., Dhekne, H. S., Lis, P., Nirujogi, R. S., Karayel, O., Tonelli, F., Martinez, T. N., Lorentzen, E., Pfeffer, S. R., Alessi, D. R., and Mann, M. (2017) Systematic proteomic analysis of LRRK2-mediated Rab GTPase phosphorylation establishes a connection to ciliogenesis. *eLife* **6,** e31012

Stenmark, H. (2009) Rab GTPases as coordinators of vesicle traffic. *Nat. Rev. Mol. Cell Biol.* **10,** 513–525

Tamura, K., Ohbayashi, N., Maruta, Y., Kanno, E., Itoh, T., and Fukuda, M. (2009) Varp is a novel Rab32/38-binding protein that regulates Tyrp1 trafficking in melanocyte. *Mol. Biol. Cell* **20,** 2900-2908

Tamura, K., Ohbayashi, N., Ishibashi, K., and Fukuda, M. (2011) Structure-function analysis of VPS9-ankyrin-repeat protein (Varp) in the trafficking of tyrosinase-related protein 1 in melanocytes. *J. Biol. Chem.* **286,** 7507-7521

Wang, T., and Hong, W. (2002) Interorganellar regulation of lysosome positioning by the Golgi apparatus through Rab34 interaction with Rab-interacting lysosomal protein. *Mol. Biol. Cell* **13,** 4317–4332

Wang, T., Wong, K. K., and Hong, W. (2004) A unique region of RILP distinguishes it from its related proteins in its regulation of lysosomal morphology and interaction with Rab7 and Rab34. *Mol. Biol. Cell* **15,** 815–826

Wang, G., Hu, H. B., Chang, Y., Huang, Y., Song, Z. Q., Zhou, S. B., Chen, L., Zhang, Y. C., Wu, M., Tu, H. Q., Yuan, J. F., Wang, N., Pan, X., Li, A. L., Zhou, T., Zhang, X. M., He, K., and Li, H. Y. (2019) Rab7 regulates primary cilia disassembly through cilia excision. *J. Cell Biol.* **218,** 4030–4041

Xu, S., Liu, Y., Meng, Q., and Wang, B. (2018) Rab34 small GTPase is required for Hedgehog signaling and an early step of ciliary vesicle formation in mouse. *J. Cell Sci.* **131,** jcs213710

Yoshimura, S. I., Egerer, J., Fuchs, E., Haas, A. K., and Barr, F. A. (2007) Functional dissection of Rab GTPases involved in primary cilium formation. *J. Cell Biol.* **178,** 363–369

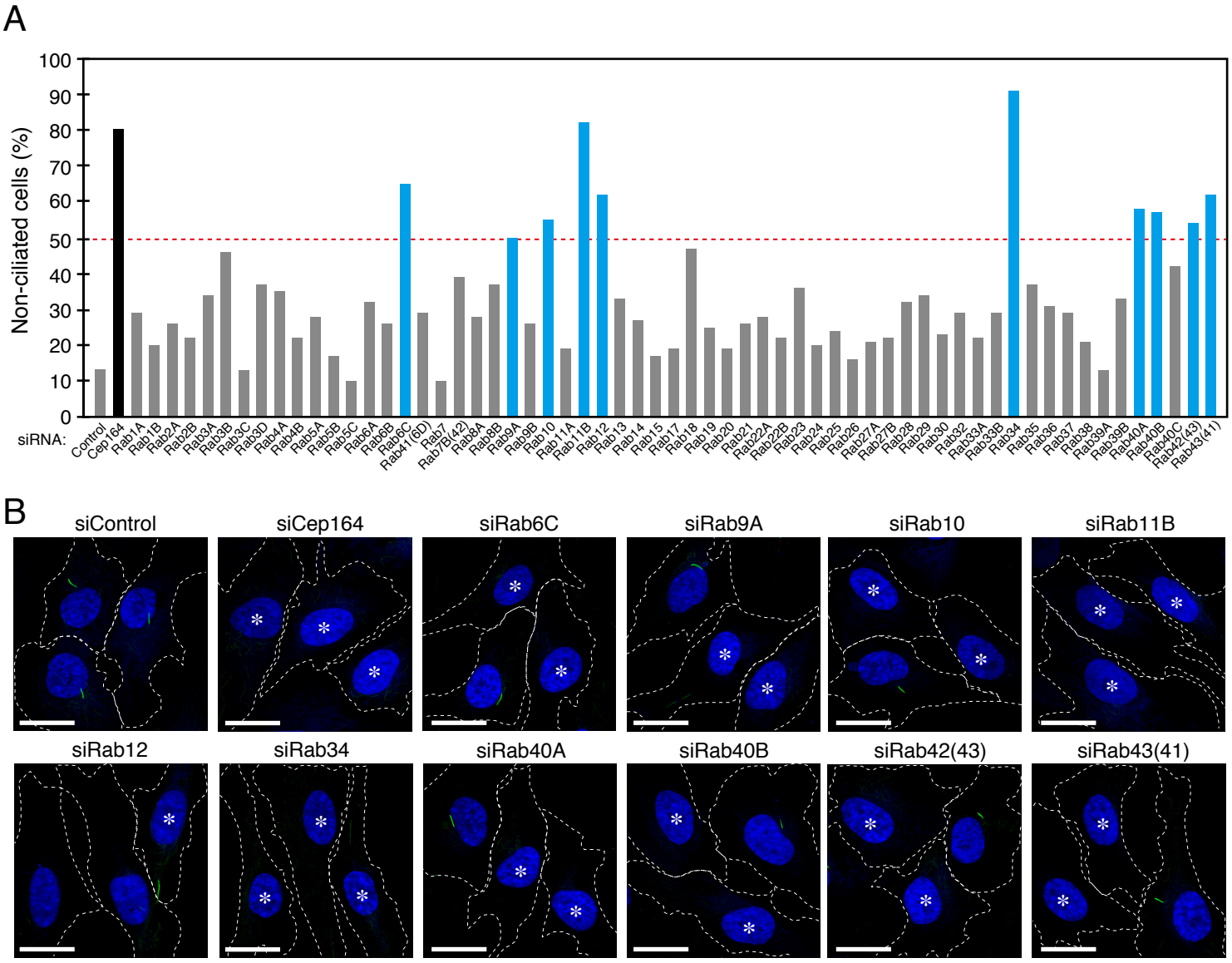

FIGURE 1. Screening for Rabs whose knockdown inhibited ciliogenesis in hTERT-RPE1 cells. *A*, the percentage of non-ciliated hTERT-RPE1 cells (%) that have been transfected with siRNA against each Rab isoform (0.2 nM) was counted after 24-h serum starvation (n >50 cells). The broken red line indicates that 50% of the cells have no cilia. The black bar represents Cep164 (positive control), and the blue bars represent candidate Rabs whose knockdown increased the number of non-ciliated cells to more than 50% compared with the control siRNA (negative control). *B*, typical images of cells transfected with control siRNA (siControl), Cep164 siRNA (siCep164) (positive control), or siRNA against candidate Rabs (siRab). The cells were fixed after 24-h serum starvation and then stained with anti-acetylated tubulin antibody (green; cilia) and DAPI (blue; nuclei). The broken white lines indicate the boundaries of each cell. *, non-ciliated cells. Scale bars, 20 μm.

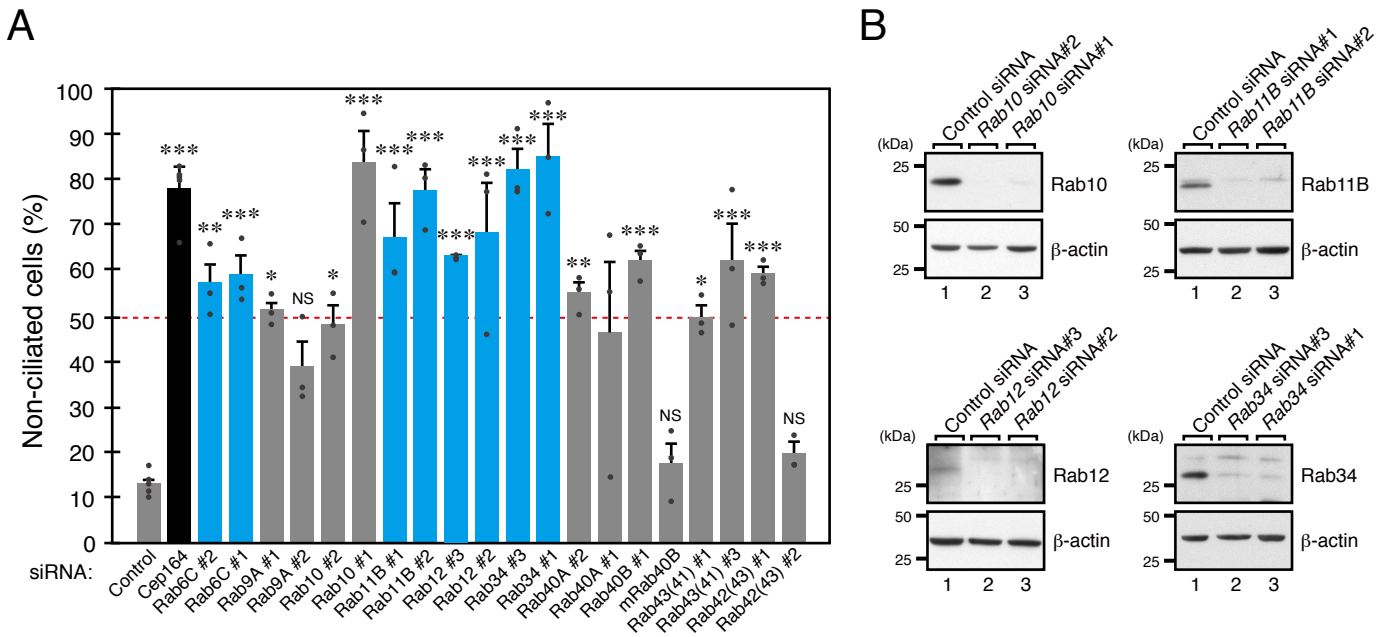

FIGURE 2. Secondary screening for Rabs whose knockdown inhibited ciliogenesis by using another siRNA site. *A*, the percentage of non-ciliated hTERT-RPE1 cells (%) transfected with the siRNAs (0.2 nM) indicated was counted after 24-h serum starvation (n >50 cells). Error bars indicate the S.E. of data from three independent experiments. The broken red line indicates that 50% of the cells have no cilia. The black bar represents Cep164 (positive control), and the blue bars represent candidate Rabs whose knockdown with two independent siRNAs increased the number of non-ciliated cells to more than 50% compared with the control siRNA (negative control). *, p <0.05; **, p <0.01; ***, p <0.001; NS, not significant compared with the control siRNA (Tukey's test). *B*, the knockdown efficiency of candidate Rabs was evaluated by immunoblotting with the antibodies indicated on the right of each panel. Cells were harvested 48 h after transfection with control siRNA or siRNA against candidate Rabs (0.2 nM). Lane 1 and lanes 2 and 3 show the results for the control siRNA and for two independent siRNAs against each Rab, respectively. The positions of the molecular mass markers (in kDa) are shown on the left.

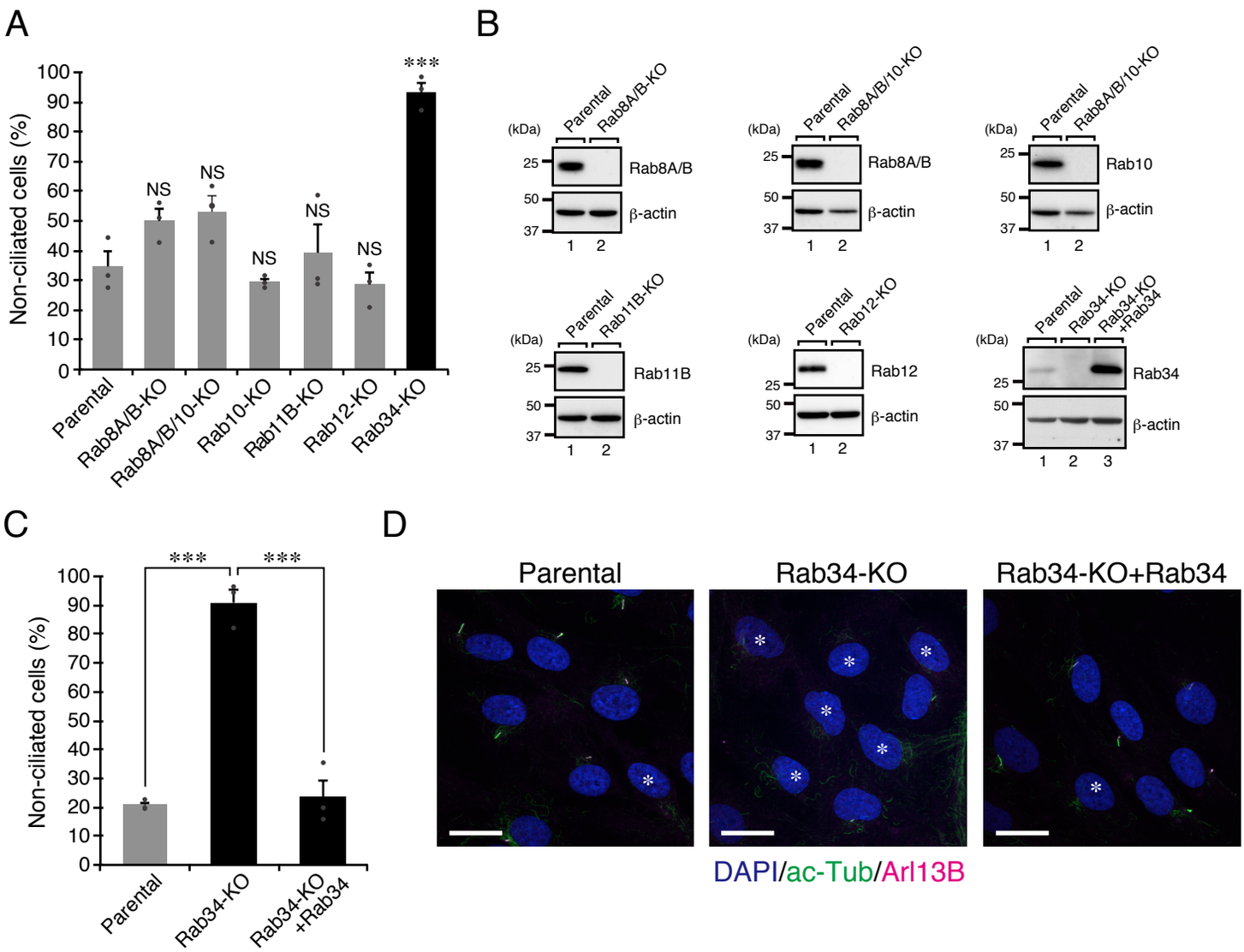

FIGURE 3. Rab34 is required for ciliogenesis in hTERT-RPE1 cells. *A*, the percentage of non-ciliated csells (%) in parental, Rab8A/B-KO, Rab10-KO, Rab8A/B/10-KO, Rab11B-KO, Rab12-KO, and Rab34-KO cells was counted after 24-h serum starvation (n >50 cells). Error bars indicate the S.E. of data from three independent experiments. ***, p <0.001; NS, not significant (Dunnett's test). *B*, the loss of Rab8A/B, Rab10, Rab11B, Rab12, or Rab34 in respective KO cells was analyzed by immunoblotting with the antibodies indicated on the right of each panel. The positions of the molecular mass markers (in kDa) are shown on the left. *C*, the percentage of non-ciliated cells (%) in parental, Rab34-KO, and stable EGFP-P2A-Rab34-expressing Rab34-KO (Rab34-KO + Rab34) cells was counted after 24-h serum starvation (n >50 cells). Error bars indicate the S.E. of data from three independent experiments. ***, p <0.001 (Tukey's test). *D*, typical images of parental, Rab34-KO, and Rab34-KO + Rab34 cells. The cells were fixed after 24-h serum starvation and then stained with anti-acetylated tubulin antibody (ac-Tub in green; cilia), anti-Arl13B antibody (magenta; cilia), and DAPI (blue; nuclei). *, non-ciliated cells. Scale bars, 20 μm.

FIGURE 4. Genomic information about the Rab-KO hTERT-RPE1 cells used in this study. The target sequences for Rab8A/B-KO, Rab10-KO, Rab8A/B/10-KO, Rab11B-KO, Rab12-KO, and Rab34-KO are shown. The green and magenta boxes indicate the PAM sequence and target sequence, respectively. The genomic mutations were checked by genomic PCR and sequencing the PCR products as described previously (Homma *et al.,* 2019), using the specific sets of oligonucleotides shown in Table 1. The donor BFP DNA was inserted into one allele of the *Rab* gene in the Rab8A/B/10-KO, Rag12-KO, and Rab34-KO cells (arrows, direction of BFP DNA).

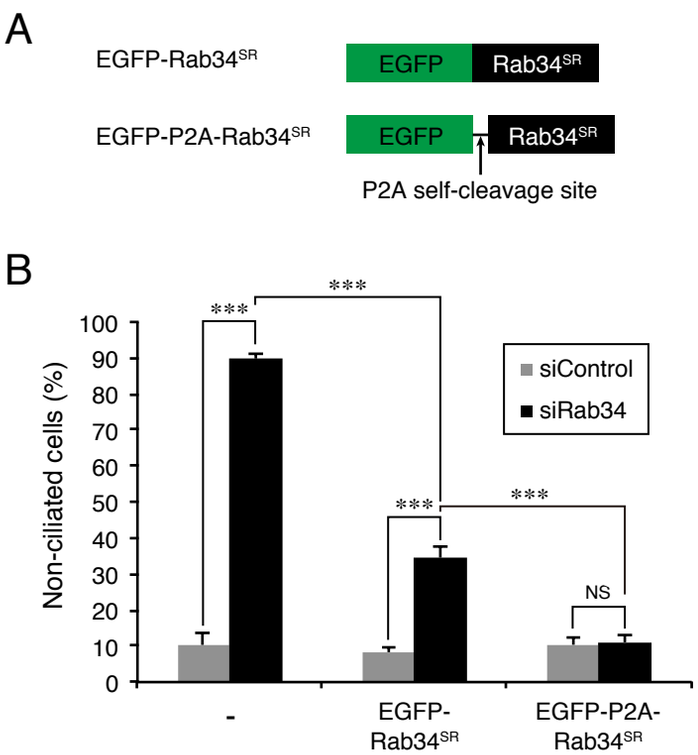

FIGURE 5. EGFP-P2A-Rab34 is more suitable for the rescue experiment than EGFP-Rab34. *A*, schematic representation of EGFP-Rab34^{SR} and EGFP-P2A-Rab34^{SR}. EGFP-P2A-Rab34^{SR} has a P2A self-cleavage site between EGFP and Rab34^{SR}. *B*, the percentage of non-ciliated cells (%) co-transfected with control siRNA (siControl) or Rab34 siRNA (siRab34: 10 nM each) and EGFP-control (-), EGFP-Rab34^{SR} or EGFP-P2A- Rab34^{SR} was counted after 24-h serum starvation (n >50 cells). Error bars indicate the SEM of data from three independent experiments. ***, p <0.001 (Tukey's test).

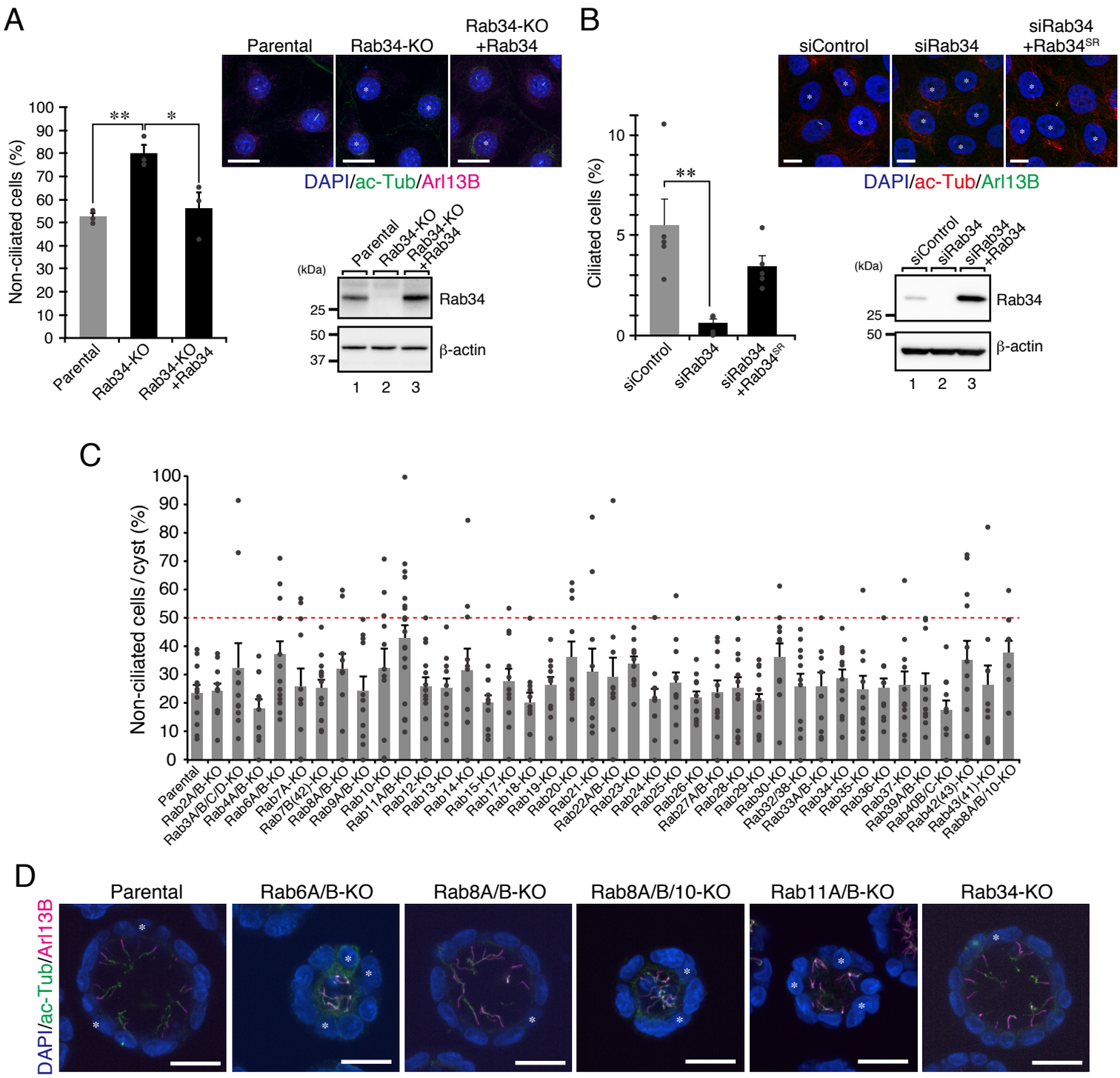
A
Parental
Rab34-KO
Rab34-KO +Rab34
Non-ciliated cells (%)
DAPI/ac-Tub/Arl13B
(kDa)
Rab34
β-actin
B
siControl
siRab34
siRab34 +Rab34SR
Ciliated cells (%)
C
Non-ciliated cells / cyst (%)
D
DAPI/ac-Tub/Arl13B
Rab6A/B-KO
Rab8A/B-KO
Rab8A/B/10-KO
Rab11A/B-KO

FIGURE 6. Rab34 is also required for ciliogenesis in NIH/3T3 cells and MCF10A cells, but not in MDCK-II cells. *A*, the percentage of non-ciliated cells (%) in the parental, Rab34-KO, and stable EGFP-P2A-Rab34-expressing Rab34-KO (Rab34-KO + Rab34) NIH/3T3 cells was counted after 48-h serum starvation (n >50 cells). Error bars indicate the S.E. of data from three independent experiments. *, p <0.05; **, p <0.01 (Tukey's test). Typical images of parental, Rab34-KO, and Rab34-KO + Rab34 cells. The cells were fixed after 48-h serum starvation and then stained with anti-acetylated tubulin antibody (ac-Tub in green; cilia), anti-Arl13B antibody (magenta; cilia), and DAPI (blue; nuclei). *, non-ciliated cells. Scale bars, 20 μm. The loss of Rab34 in KO cells was confirmed by immunoblotting with the antibodies indicated on the right of each panel. The positions of the molecular mass markers (in kDa) are shown on the left. *B*, the percentage of ciliated cells (%) in the control (siControl), Rab34-KD (siRab34), and stable EGFP-P2A-Rab34-expressing Rab34-KD (siRab34 + Rab34) MCF10A cells was counted after 24-h serum starvation (n >500 cells). Error bars indicate the S.E. of data from five independent experiments. **, p <0.01 (Tukey's test). The cells were fixed after 24-h serum starvation and then stained with anti-acetylated tubulin antibody (ac-Tub in red; cilia), anti-Arl13B antibody (green; cilia), and DAPI (blue; nuclei). *, non-ciliated cells. Scale bars, 10 μm. The knockdown efficiency of Rab34 was evaluated by immunoblotting with the antibodies indicated on the right of each panel. Cells were harvested 72 h after transfection with control siRNA (siControl) or Rab34 siRNA (siRab34). The positions of the molecular mass markers (in kDa) are shown on the left. *C*, the percentage of non-ciliated cells per cyst (%) in parental and Rab-KO MDCK-II cells was counted after 7-day culture in collagen gel. Note that the percentage of non-ciliated cells of all of the Rab-KO cysts was below 50% (indicated as a broken red line). Error bars indicate the S.E. of data from at least ten cysts. *D*, typical images of parental, Rab6A/B-KO, Rab8A/B-KO, Rab8A/B/10-KO, Rab11A/B-KO, and Rab34-KO MDCK-II cells. The cells were fixed after 7-day culture in collagen gel and then stained with anti-acetylated tubulin antibody (ac-Tub in green; cilia), anti-Arl13B antibody (magenta; cilia), and DAPI (blue; nuclei). *, non-ciliated cells. Scale bars, 20 μm.

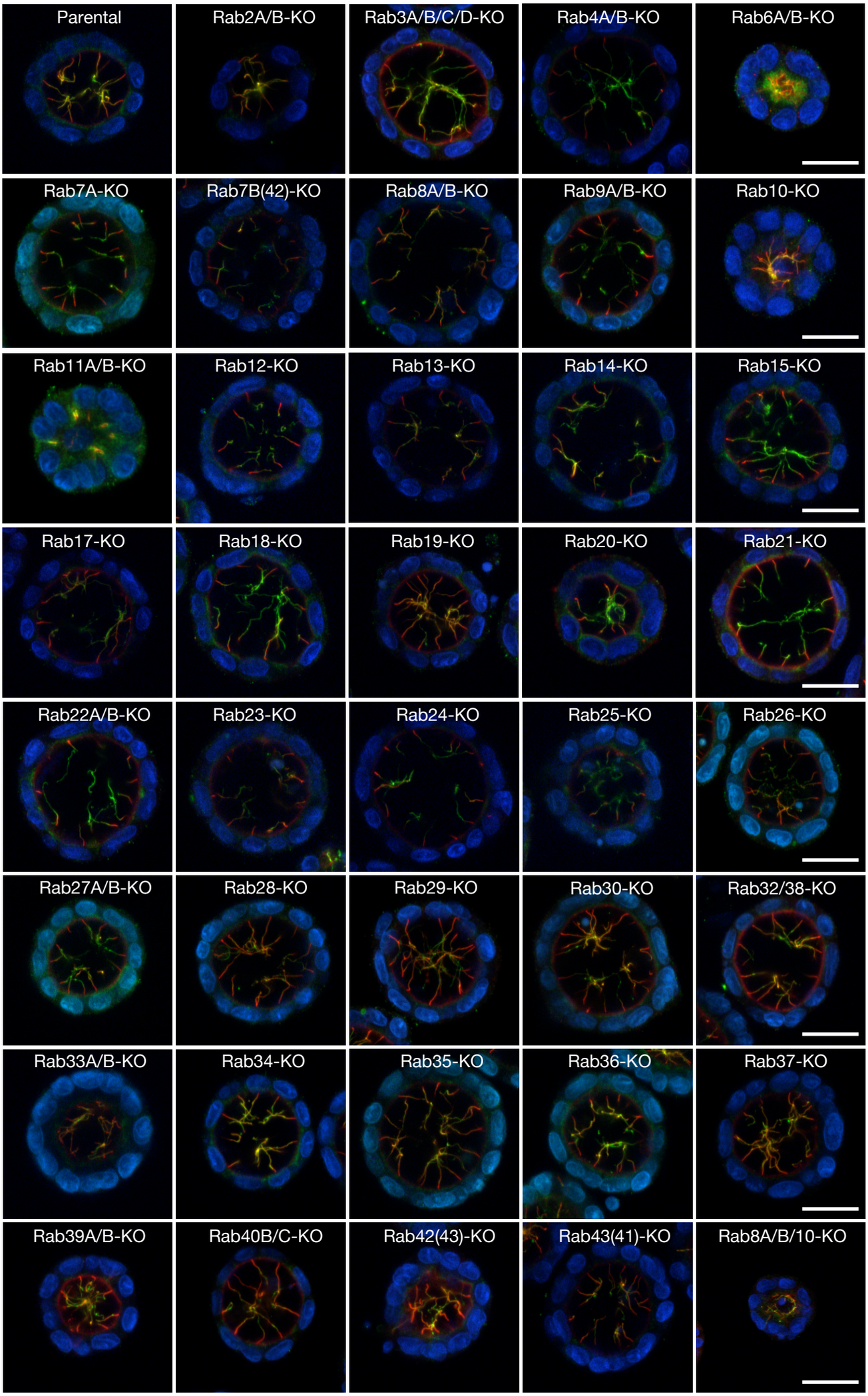
Parental
Rab2A/B-KO
Rab3A/B/C/D-KO
Rab4A/B-KO
Rab6A/B-KO
Rab7A-KO
Rab7B(42)-KO
Rab8A/B-KO
Rab9A/B-KO
Rab10-KO
Rab11A/B-KO
Rab12-KO
Rab13-KO
Rab14-KO
Rab15-KO
Rab17-KO
Rab18-KO
Rab19-KO
Rab20-KO
Rab21-KO
Rab22A/B-KO
Rab23-KO
Rab24-KO
Rab25-KO
Rab26-KO
Rab27A/B-KO
Rab28-KO
Rab29-KO
Rab30-KO
Rab32/38-KO
Rab33A/B-KO
Rab34-KO
Rab35-KO
Rab36-KO
Rab37-KO
Rab39A/B-KO
Rab40B/C-KO
Rab42(43)-KO
Rab43(41)-KO
Rab8A/B/10-KO

FIGURE 7. Effect of Rab-KO on ciliogenesis in MDCK-II cells. Typical images of parental and Rab-KO cysts of MDCK-II cells (Homma *et al.,* 2019). Cysts grown in collagen gel for 7 days were fixed with TCA (trichloroacetic acid) and then stained with anti-acetylated tubulin antibody (*green*; cilia), anti-Arl13B antibody (*magenta*; cilia), and DAPI (*blue*; nuclei). Scale bars, 20 μm.

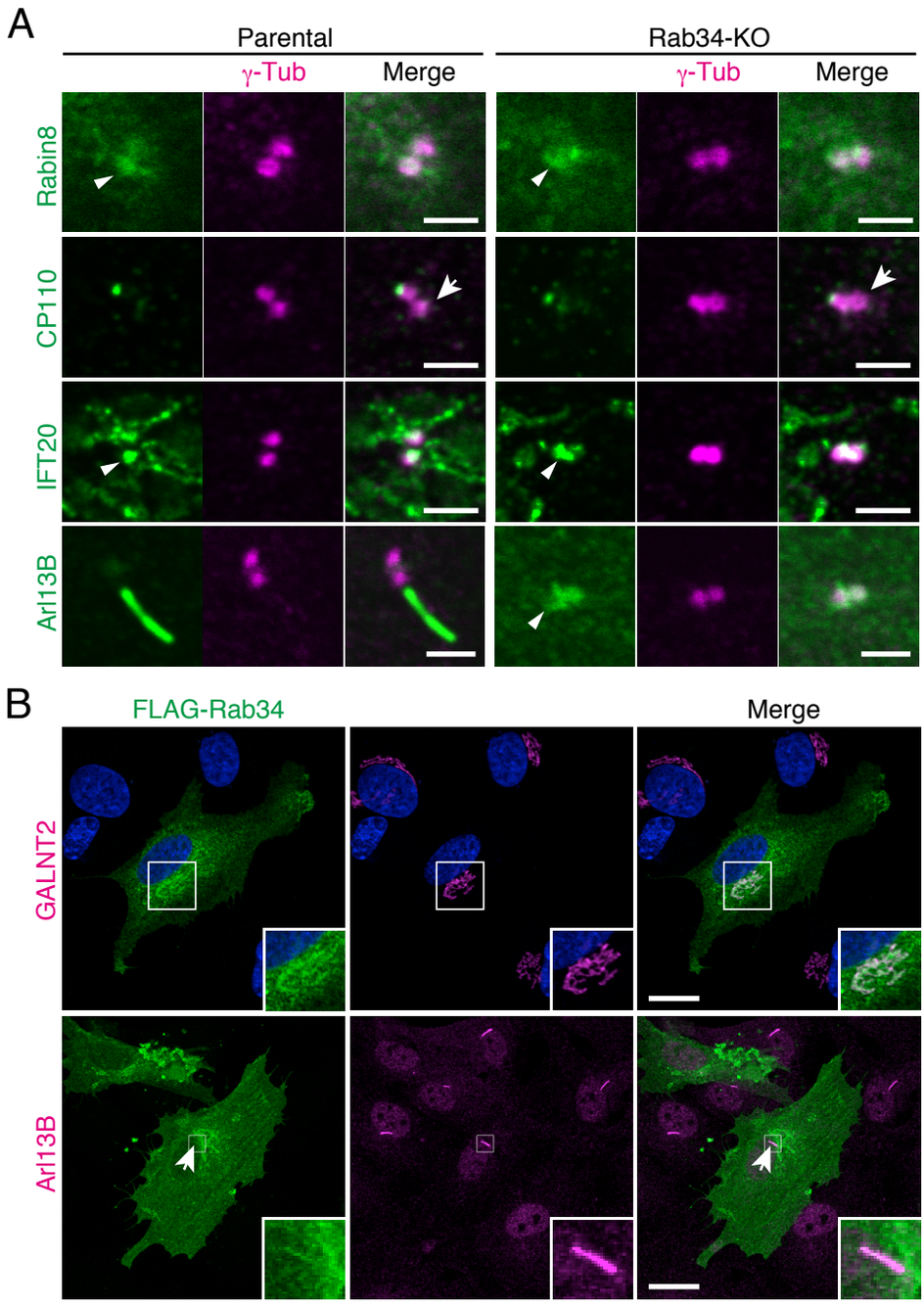

FIGURE 8. Rab34 is required for early steps in serum-starvation-induced ciliogenesis in hTERT-RPE1 cells. *A*, typical Rabin8, CP110, IFT20, and Arl13B images of parental and Rab34-KO cells. For Rabin8 staining, cells stably expressing EGFP-Rabin8 (green) were fixed after 1-h serum starvation and then stained with anti-γ-tubulin antibody (γ-Tub in magenta; centrioles) (top panels). For CP110, IFT20, and Arl13B staining, cells were fixed after 24-h serum starvation and then stained with antibodies against CP110 (green) and γ-tubulin (magenta) (second panels), IFT20 (green) and γ-tubulin (magenta) (third panels), or Arl13B (green) and γ-tubulin (magenta) (bottom panels). The arrows and arrowheads indicate CP110-negative centrioles and centriole-localized Rabin8 (IFT20 or Arl13B), respectively. Scale bars, 2 μm. *B*, typical images of FLAG-Rab34 and GALNT2 or Arl13B in hTERT-RPE1 cells expressing FLAG-Rab34 (WT). For GALNT2 staining, cells were fixed without serum starvation and stained with antibodies against GALNT2 (magenta) and FLAG (green in top panels). For Arl13B staining, cells were fixed after 24-h serum starvation and then stained with antibodies against Arl13B (magenta) and FLAG (green in bottom panels). The arrows indicate FLAG-Rab34-positive primary cilia. Scale bars, 20μm.

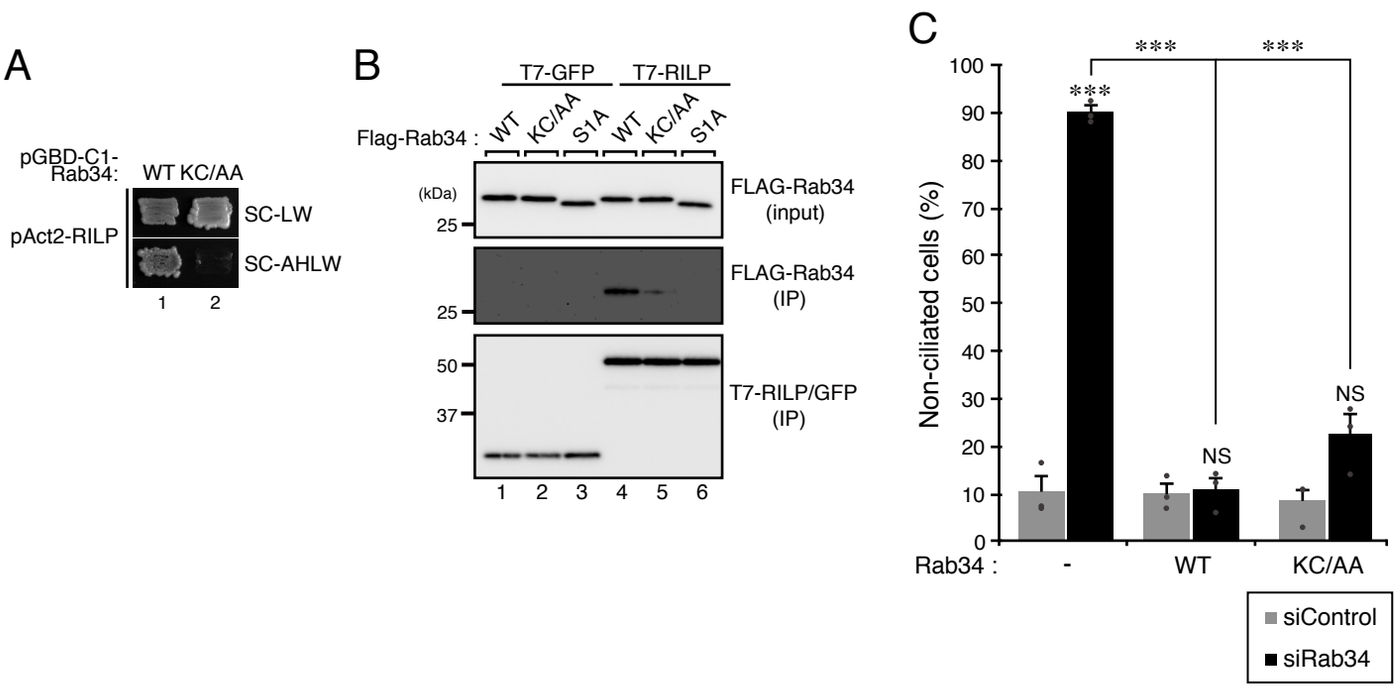

FIGURE 9. Rab34 (K115A/C116A) rescued the Rab34-KD phenotype. *A*, interaction between Rab34(KC/AA) and RILP was analyzed by yeast two-hybrid assays. Yeast cells expressing pGBD-C1-Rab34(WT) or -Rab34(KC/AA) and pAct2-RILP were streaked on SC-LW (upper panel) and SC-AHLW plate (lower panel; selection medium) and incubated at 30ºC. *B*, interaction between Rab34(WT), Rab34(KC/AA), or Rab34(S1A) and RILP was analyzed by co-immunoprecipitation in COS7 cells. COS7 cell lysates expressing FLAG-tagged Rab34(WT), Rab34(KC/AA), or Rab34(S1A) and T7-tagged GFP or RILP were incubated with anti-T7-tag-antibody-conjugated agarose beads. Proteins bound to the beads (*IP*) and a 1% volume of total cell lysates (input) were analyzed by immunoblotting with HRP-conjugated anti-FLAG and anti-T7 tag antibodies indicated on the right of each panel. The positions of the molecular mass markers (in kDa) are shown on the left. C, the percentage of non-ciliated cells (%) in cells stably expressing Rab34(WT) or Rab34(KC/AA) that had been transfected with control siRNA (siControl) or Rab34 siRNA (siRab34: 10 nM each)was counted after 24-h serum starvation (n >50 cells) . Error bars indicate the S.E. of data from three independent experiments. ***, p <0.001; NS, not significant (Tukey's test).

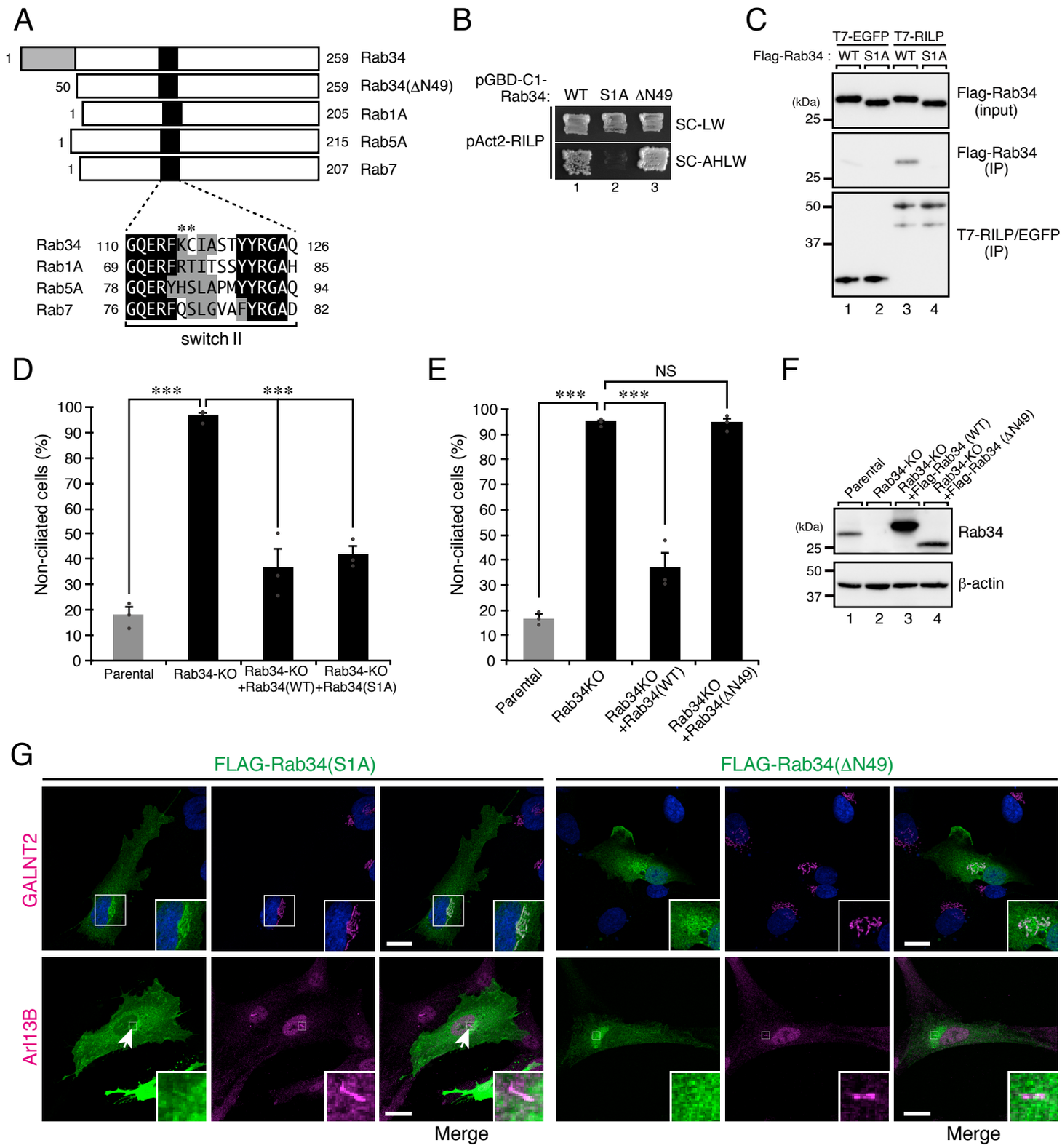
A
1
259
Rab34
50
259
Rab34(ΔN49)
1
205
Rab1A
1
215
Rab5A
1
207
Rab7
**
Rab34 110 GQERFKCIASTYYRGAQ 126
Rab1A 69 GQERFRTITSSYYRGAH 85
Rab5A 78 GQERYHSLAPMYYRGAQ 94
Rab7 76 GQERFQSLGVAFYRGAD 82
switch II
B
pGBD-C1-Rab34:
WT
S1A
ΔN49
pAct2-RILP
SC-LW
SC-AHLW
1
2
3
C
T7-EGFP
T7-RILP
Flag-Rab34 :
WT
S1A
WT
S1A
(kDa)
25
Flag-Rab34 (input)
25
Flag-Rab34 (IP)
50
37
T7-RILP/EGFP (IP)
1
2
3
4
D
Non-ciliated cells (%)
***
***
Parental
Rab34-KO
Rab34-KO +Rab34(WT)
Rab34-KO +Rab34(S1A)
E
Non-ciliated cells (%)
NS
***
***
Parental
Rab34KO
Rab34KO +Rab34(WT)
Rab34KO +Rab34(ΔN49)
F
Parental
Rab34-KO
Rab34-KO +Flag-Rab34 (WT)
Rab34-KO +Flag-Rab34 (ΔN49)
(kDa)
25
Rab34
50
37
β-actin
1
2
3
4
G
FLAG-Rab34(S1A)
FLAG-Rab34(ΔN49)
GALNT2
Arl13B
Merge
Merge

FIGURE 10. The unique long N-terminal region of Rab34, not its specific sequence in the switch II region, is required for ciliogenesis in hTERT-RPE1 cells. *A*, schematic representation of mouse Rab1A, Rab5A, Rab7, and Rab34 (WT and ΔN49), and sequence alignment of the switch II region (black boxes) of mouse Rab1A, Rab5A, Rab7, and Rab34. Identical and similar residues in the switch II region are shown against a black background and a gray background, respectively. The Lys-115 and Cys-116 of Rab34 (asterisks) are not conserved in other Rabs except Rab36 (Matsui *et al.*, 2012). The unique long N-terminal region of Rab34 is indicated by a gray box. *B*, interaction between Rab34(WT), Rab34(S1A), or Rab34(ΔN49) and RILP was analyzed by yeast two-hybrid assays. Yeast cells expressing pGBD-C1-Rab34(WT), Rab34(S1A), or Rab34(ΔN49) and pAct2-RILP were streaked on an SC-LW plate (upper panel) and on an SC-AHLW plate (lower panel: selection medium) and incubated at 30ºC. *C*, interaction between Rab34(WT) or Rab34(S1A) and RILP was analyzed by co-immunoprecipitation assays of COS7 cell lysates. COS7 cell lysates expressing FLAG-tagged Rab34(WT) or Rab34(S1A) and T7-tagged EGFP or RILP were incubated with anti-T7-tag-antibody-conjugated agarose beads. Proteins bound to the beads (IP) and a 1% volume of total cell lysates (input) were analyzed by immunoblotting with the HRP-conjugated anti-FLAG and anti-T7 tag antibodies indicated on the right of each panel. The positions of the molecular mass markers (in kDa) are shown on the left. *D*, the percentage of non-ciliated cells (%) in parental, Rab34-KO, and stable tagless Rab34(WT)-expressing or Rab34(S1A)-expressing Rab34-KO cells (Rab34-KO + Rab34(WT) or Rab34(S1A)) was counted after 24-h serum starvation (n >50 cells). Error bars indicate the S.E. of data from three independent experiments. ***, p <0.001 (Tukey's test). *E*, the percentage of non-ciliated cells (%) in parental, Rab34-KO, and stable FLAG-Rab34(WT), -Rab34(ΔN49)-expressing Rab34-KO cells (Rab34-KO + Rab34(WT), or Rab34(ΔN49)) was counted after 24-h serum starvation (n >50 cells). Error bars indicate the S.E. of data from three independent experiments. ***, p <0.001; NS, not significant (Tukey's test). *F*, the protein expression levels of FLAG-tagged Rab34(WT) and Rab34(ΔN49) in *E* were analyzed by immunoblotting with the antibodies indicated on the right of each panel. The positions of the molecular mass markers (in kDa) are shown on the left. *G*, typical images of FLAG-Rab34 and GALNT2 or Arl13B in hTERT-RPE1 cells expressing FLAG-Rab34(S1A) or -Rab34(ΔN49). For GALNT2 staining, cells not subjected to serum starvation were fixed and stained with anti-GALNT2 antibody (magenta), anti-FLAG tag antibody (green), and DAPI (blue in top panels). For Arl13B staining, cells were fixed after 24-h serum starvation and then stained with antibodies against Arl13B (magenta) and FLAG (green in bottom panels). The arrows indicate FLAG-Rab34-positive primary cilia. Scale bars, 20 μm.

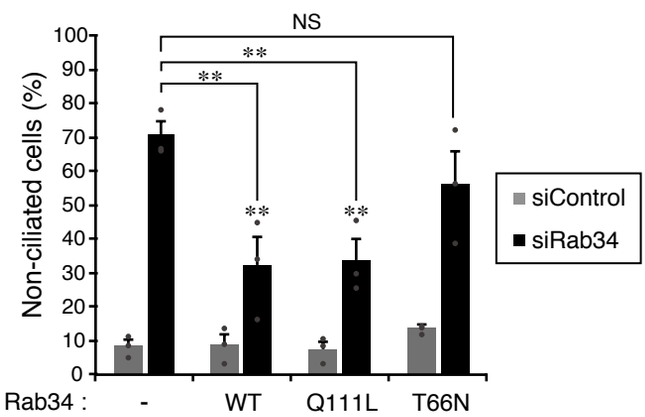

FIGURE 11. Active Rab34 is required for ciliogenesis in hTERT-RPE1 cells. *A*, the percentage of non-ciliated cells (%) in cells stably expressing Rab34(WT), Rab34(Q116L), or Rab34(T66N) was counted after 24-h serum starvation (n >50 cells) that had been transfected with control siRNA (siControl) or Rab34 siRNA (siRab34). Error bars indicate the S.E. of data from three independent experiments. **, p <0.01; NS, not significant (Tukey's test).

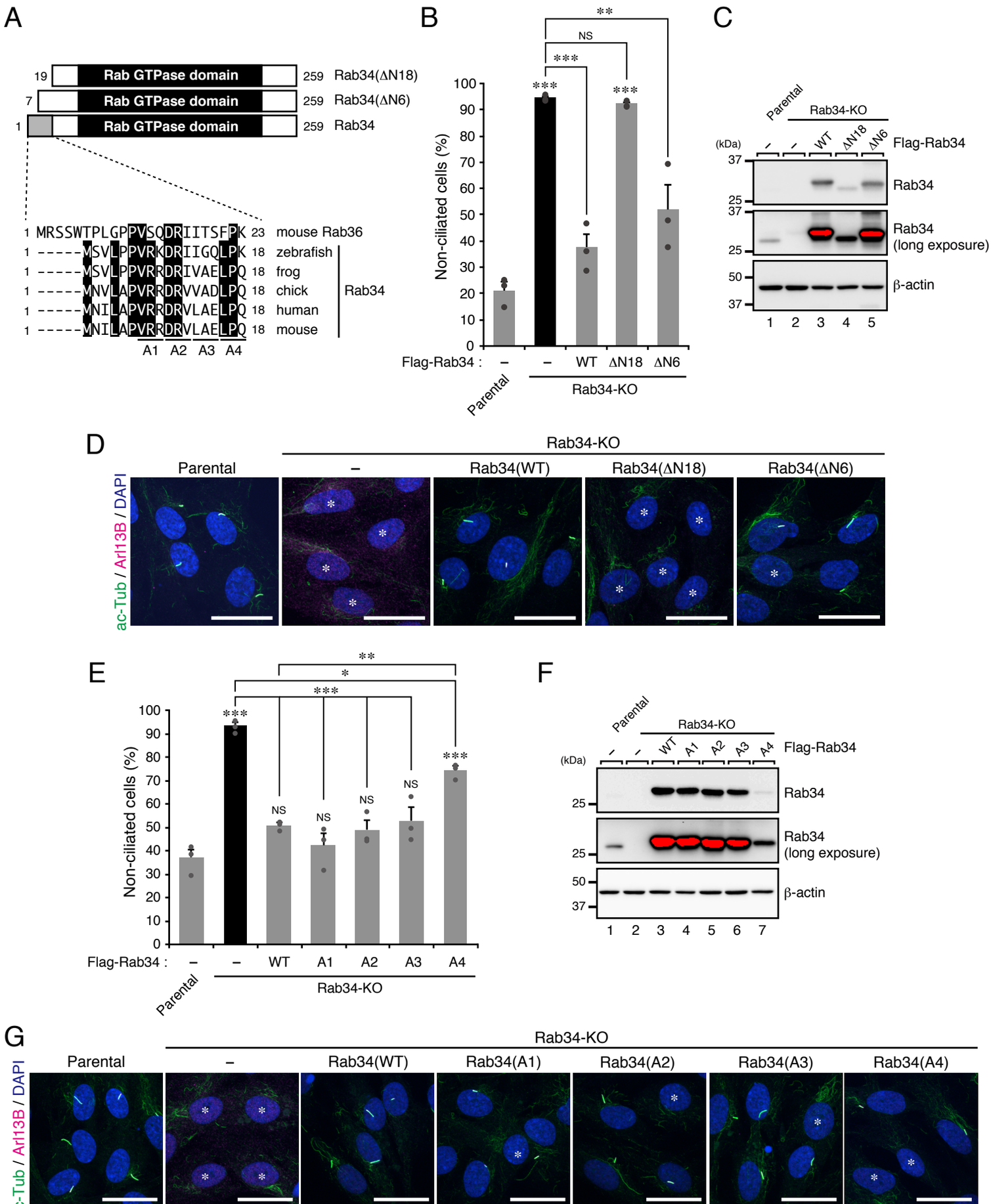
A
Rab GTPase domain
Rab34(ΔN18)
Rab34(ΔN6)
Rab34
mouse Rab36
zebrafish
frog
chick
human
mouse
Rab34
A1 A2 A3 A4
B
Non-ciliated cells (%)
Flag-Rab34 :
Parental
Rab34-KO
WT
ΔN18
ΔN6
NS
C
Parental
Rab34-KO
(kDa)
Flag-Rab34
Rab34
Rab34 (long exposure)
β-actin
D
Parental
Rab34-KO
Rab34(WT)
Rab34(ΔN18)
Rab34(ΔN6)
ac-Tub / Arl13B / DAPI
E
Non-ciliated cells (%)
Flag-Rab34 :
Parental
Rab34-KO
WT
A1
A2
A3
A4
NS
F
Parental
Rab34-KO
(kDa)
Flag-Rab34
Rab34
Rab34 (long exposure)
β-actin
G
Parental
Rab34-KO
Rab34(WT)
Rab34(A1)
Rab34(A2)
Rab34(A3)
Rab34(A4)
ac-Tub / Arl13B / DAPI

FIGURE 12. Amino acid numbers 16–18 of Rab34 required for ciliogenesis in hTERT-RPE1 cells. *A,* schematic representation of mouse Rab34(WT), Rab34(ΔN18), and Rab34(ΔN6), and sequence alignment of the N-terminal region (gray box) of zebrafish, african clawed frog, chick, human, and mouse Rab34 and mouse Rab36. Identical residues in their N-terminal region are shown against a black background. The Rab GTPase domain of Rab34 is indicated by a black box. *B,* the percentage of non-ciliated cells (%) in parental, Rab34-KO, and Rab34-KO cells stably expressing FLAG-Rab34(WT), Rab34(ΔN18), or Rab34(ΔN6) was counted after 24-h serum starvation (n >50 cells). Error bars indicate the S.E. of data from three independent experiments. **, p <0.01; ***, p <0.001; NS, not significant (Tukey's test). *C,* the protein expression levels of FLAG-tagged Rab34(WT), Rab34(ΔN18), and Rab34(ΔN6) in *B* were analyzed by immunoblotting with the antibodies indicated on the right of each panel. The positions of the molecular mass markers (in kDa) are shown on the left. *D,* typical images of parental, Rab34-KO, and Rab34-KO + Flag-Rab34(WT), Rab34(ΔN18), or Rab34(ΔN6) cells. The cells were fixed after 24-h serum starvation and then stained with anti-ac-Tub antibody (green; cilia), anti-Arl13B antibody (magenta; cilia), and DAPI (blue; nuclei). *, non-ciliated cells. Scale bars, 20 μm. *E,* the percentage of non-ciliated cells (%) in parental, Rab34-KO, and Rab34-KO cells stably expressing FLAG-Rab34 (WT), Rab34(A1), Rab34(A2), Rab34(A3), or Rab34(A4) was counted after 24-h serum starvation (n >50 cells). Error bars indicate the S.E. of data from three independent experiments. *, p <0.05; **, p < 0.01; ***, p <0.001; NS, not significant (Tukey's test). *F,* the protein expression levels of FLAG-tagged Rab34(WT), Rab34(A1), Rab34(A2), Rab34 (A3), and Rab34(A4) in *E* were analyzed by immunoblotting with the antibodies indicated on the right of each panel. The positions of the molecular mass markers (in kDa) are shown on the left. *G,* typical images of parental, Rab34-KO, and Rab34-KO + Flag-Rab34(WT), Rab34(A1), Rab34(A2), Rab34(A3), or Rab34(A4) cells. The cells were fixed after 24-h serum starvation and then stained with anti-ac-Tub antibody (green; cilia), anti-Arl13B antibody (magenta; cilia), and DAPI (blue; nuclei). *, non-ciliated cells. Scale bars, 20 μm.

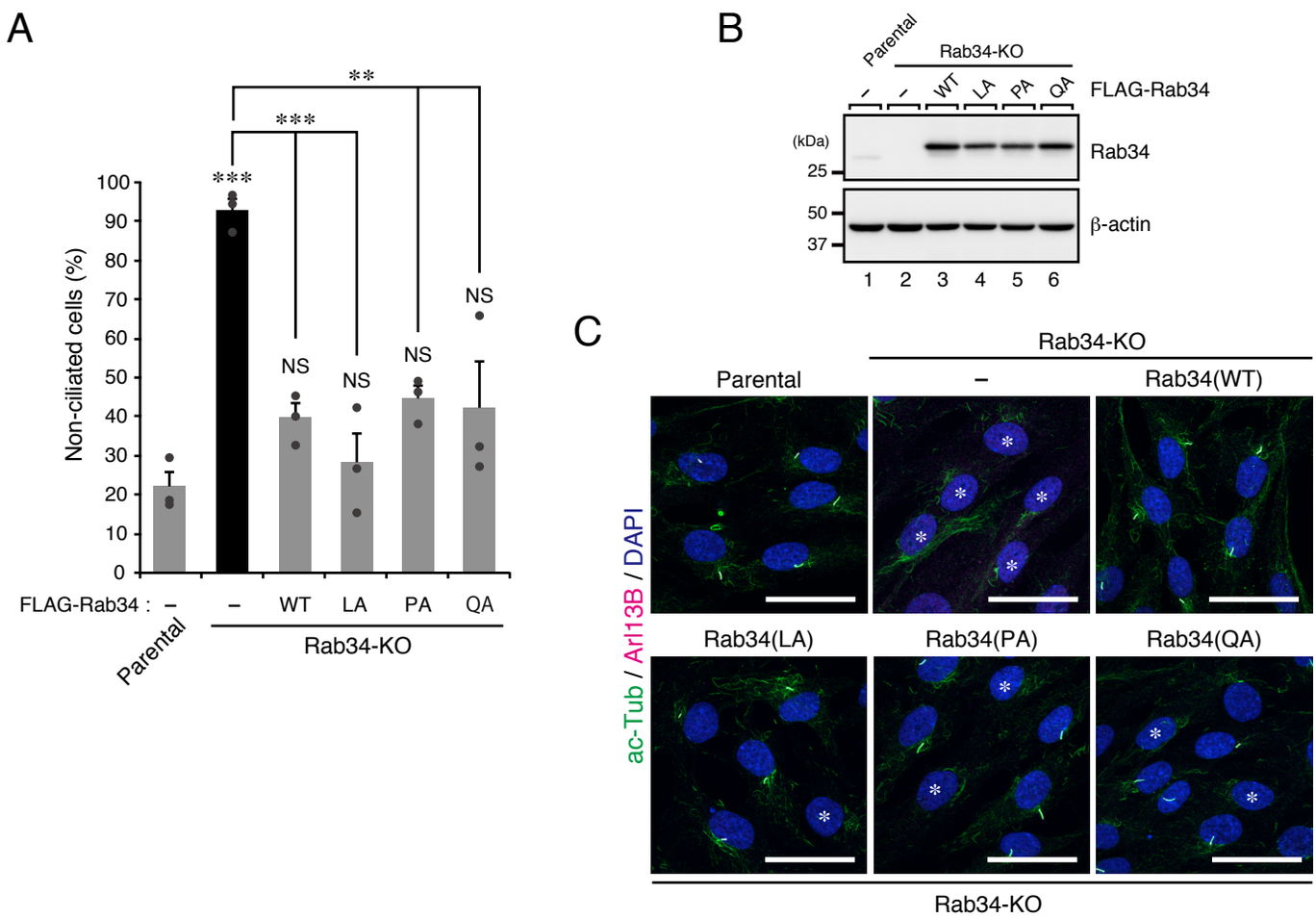

FIGURE 13. Single Ala mutants in the LPQ sequence of Rab34 completely rescued the Rab34-KO phenotype. *A*, the percentage of non-ciliated cells (%) in parental, Rab34-KO, and Rab34-KO cells stably expressing FLAG-Rab34 (WT), Rab34(LA), Rab34(PA), or Rab34(QA) was counted after 24-h serum starvation (n >50 cells). Error bars indicate the S.E. of data from three independent experiments. **, $p < 0.01$; ***, $p < 0.001$; NS, not significant (Tukey's test). *B*, the protein expression levels of FLAG-tagged Rab34(WT), Rab34(LA), Rab34(PA), and Rab34(QA) in *A* were analyzed by immunoblotting with the antibodies indicated on the right of each panel. The positions of the molecular mass markers (in kDa) are shown on the left. *C*, typical images of parental, Rab34-KO, Rab34-KO + Rab34(WT), Rab34-KO + Rab34 (LA), Rab34-KO + Rab34(PA), and Rab34-KO + Rab34(QA) cells. The cells were fixed after 24-h serum starvation and then stained with anti-ac-Tub antibody (green; cilia), anti-Arl13B antibody (magenta; cilia), and DAPI (blue; nuclei). *, non-ciliated cells. Scale bars, 20 μm.

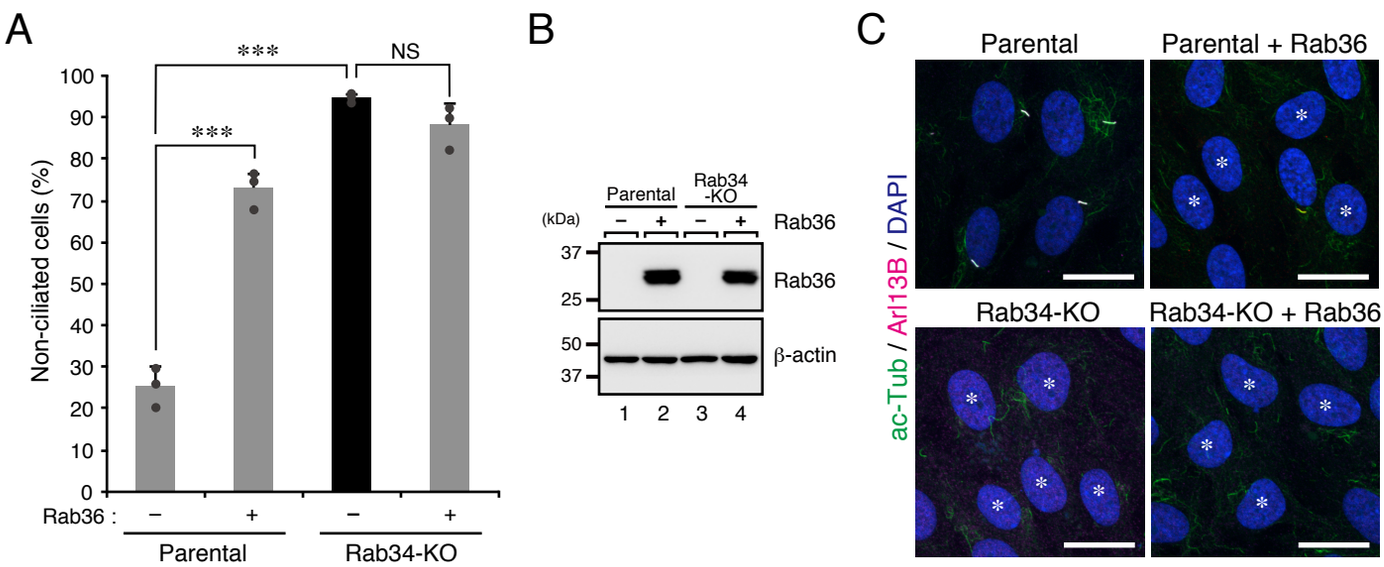

FIGURE 14. Rab36 failed to rescue the Rab34-KO phenotype. *A,* the percentage of non-ciliated cells (%) in parental and parental cells stably expressing Rab36, and Rab34-KO and Rab34-KO cells stably expressing Rab36 was counted after 24-h serum starvation (n >50 cells). Error bars indicate the S.E. of data from three independent experiments. ***, p <0.001; NS, not significant (Tukey's test). *B,* the protein expression level of Rab36 in *A* was analyzed by immunoblotting with the antibodies indicated on the right of each panel. The positions of the molecular mass markers (in kDa) are shown on the left. *C,* typical images of parental, parental + Rab36, Rab34-KO, and Rab34-KO + Rab36 cells. The cells were fixed after 24-h serum starvation and then stained with anti-ac-Tub antibody (green; cilia), anti-Arl13B antibody (magenta; cilia), and DAPI (blue; nuclei). *, non-ciliated cells. Scale bars, 20 μm.

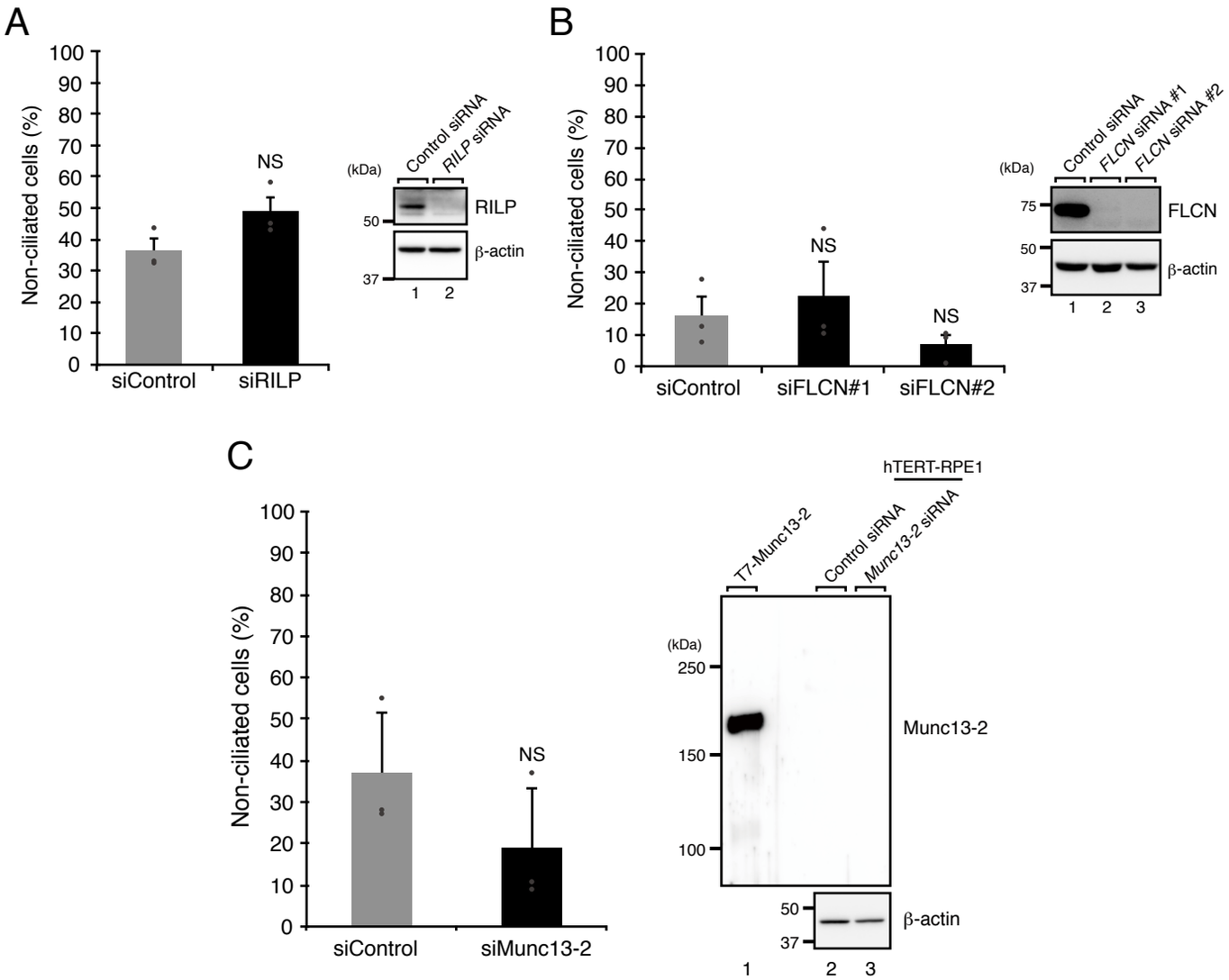

FIGURE 15. The known Rab34-interacting proteins, RILP, FLCN, and Munc13-2, are not required for ciliogenesis in hTERT-RPE1 cells. *A*, the percentage of non-ciliated control cells (siControl: 0.2 nM) and RILP-KD (siRILP: 0.2 nM) hTERT-RPE1 cells (%) was counted after 24-h serum starvation (n >50 cells). Error bars indicate the S.E. of data from three independent experiments. NS, not significant (Student's unpaired *t*-test). The knockdown efficiency of RILP was evaluated by immunoblotting with the antibodies indicated on the right of each panel. Cells were harvested 48 h after transfection with control siRNA or RILP siRNA. The positions of the molecular mass markers (in kDa) are shown on the left. The asterisk indicates non-specific bands of the anti-RILP antibody. *B*, the percentage of non-ciliated control cells (siControl: 10 nM) and FLCN-KD (siFLCN#1 and #2: 10 nM) hTERT-RPE1 cells (%) was counted after 24-h serum starvation (n >50 cells). Error bars indicate the S.E. of data from three independent experiments. NS, not significant (Tukey's test). The knockdown efficiency of FLCN was evaluated by immunoblotting with the antibodies indicated on the right of each panel. Cells were harvested 48 h after transfection with control siRNA or FLCN siRNA. Lane 1 shows the results obtained with control cells, and lanes 2 and 3 show the results obtained with the two FLCN-KD cells. The positions of the molecular mass markers (in kDa) are shown on the left. *C*, the percentage of non-ciliated cells (%) in cells that had been transfected with control siRNA (siControl) or Munc13-2 siRNA (siMunc13-2: 10 nM each) was counted after 24-h serum starvation (n >50 cells). Error bars indicate the S.E. of data from three independent experiments. NS, not significant (Student's unpaired *t*-test). Endogenous expression of Munc13-2 in hTERT-RPE1 cells was analyzed by immunoblotting with the antibodies indicated on the right of each panel. Lane 1 shows Munc13-2 protein that was overexpressed in COS7 cells and immunoprecipitated with anti-T7-tag-antibody-conjugated agarose beads. Lanes 2 and 3 show hTERT-RPE1 cells that had been treated with the control siRNA (*siControl*) and Munc13-2 siRNA (*siMunc13-2*: 10 nM each), respectively. The positions of the molecular mass markers (in kDa) are shown on the left.

Table 1. A list of the primers and siRNAs used in this study

Primer Name	Sequence
P2A-5'	GATCTGGAAGCGGAGCTACTAACTTCAGCCTGCTGAAGCAG GCTGGAGACGTGGAGGAGAACCCTGGACCTGGATCCTGACC GC
P2A-3'	GGTCAGGATCCAGGTCCAGGGTTCTCCTCCACGTCTCCAGCC TGCTTCAGCAGGCTGAAGTTAGTAGCTCCGCTTCCA
humanRab34-SR1-5'	GGATCCATGAACATTCTGGCACCCGTG
humanRab34-SR1-3'	CCACTCCAATGGTGGCCTTGTAGTTTTTGTCGAAAGTATCCT T
Rab34-KC/AA-5'	CAGGAAAGGTTCGCGGCCATTGCTTCCACCTA
Rab34-KC/AA-3'	TAGGTGGAAGCAATGGCCGCGAACCTTTCCTG
Rab34-S1A-5'	CGAACAATTACTTCCAGTTACTACCGTGGAGCTCATGCCATC ATCATTG
Rab34-S1A-3'	GAACCTTTCCTGACCAGCCGTGTCC
Rab34-ΔN49-5'	ATGGATCCATGTTTAAGATATCCAAGGTC
Rab34-ΔN18-5'	ATGGATCCATGTGCCTGAAGAAAGAGGCCG
Rab34-ΔN6-5'	ACGGATCCATGGTGCGGAGGGACCGCGTCC
Rab34-A1-5'	ACGGATCCATGAACATTCTGGCGCCCGCGGCGGCGGACCGC GTCCTGGCGGAGCTGCCCCAGTGCCTG
Rab34-A2-5'	ACGGATCCATGAACATTCTGGCGCCCGTGCGGAGGGCCGCC GCCCTGGCGGAGCTGCCCCAGTGCCTG
Rab34-A3-5'	ACGGATCCATGAACATTCTGGCGCCCGTGCGGAGGGACCGC GTCGCGGCGGCGCTGCCCCAGTGCCTG
Rab34-A4-5'	ACGGATCCATGAACATTCTGGCGCCCGTGCGGAGGGACCGC GTCCTGGCGGAGGCGGCCGCGTGCCTG
Rab34-LA-5'	ACGGATCCATGAACATTCTGGCGCCCGTGCGGAGGGACCGC GTCCTGGCGGAGGCGCCCCAGTGCCTG
Rab34-PA-5'	ACGGATCCATGAACATTCTGGCGCCCGTGCGGAGGGACCGA GTCCTGGCGGAGCTGGCCCAGTGCCTG
Rab34-QA-5'	ACGGATCCATGAACATTCTGGCGCCCGTGCGGAGGGACCGC GTCCTGGCGGAGCTGCCCGCGTGCCTG
Rab8A-gRNA-5'	CACCGATTAGGACCATAGAGCTCGA
Rab8A-gRNA-3'	AAACTCGAGCTCTATGGTCCTAATC
Rab8B-gRNA-5'	CACCGCTCCTGCTGATCGGCGACTC
Rab8B-gRNA-3'	AAACGAGTCGCCGATCAGCAGGAGC
Rab10-gRNA-5'	CACCGTTTCAAGCTGCTCCTGATCG
Rab10-gRNA-3'	AAACCGATCAGGAGCAGCTTGAAAC
Rab10-gRNA-Donor-3'	TCCACGATCAGGAGCAGCTTGAAAC
Rab11B-gRNA-5'	CACCGTCTCCAGGTTGAACTCGTTG
Rab11B-gRNA-3'	AAACCAACGAGTTCAACCTGGAGAC
Rab12-gRNA-5'	CACCGATCCGGGCGCCGCGCTGCAG
Rab12-gRNA-3'	AAACCTGCAGCGCGGCGCCCGGATC
Rab12-gRNA-Donor-3'	TCCAAGACCGCCGCCGCCCCCGGCC
Rab34-gRNA-5'	CACCGACATTCTGGCACCCGTGCGG
Rab34-gRNA-3'	AAACCCGCACGGGTGCCAGAATGTC
Rab34-gRNA-Donor-3'	TCCACCGCACGGGTGCCAGAATGTC
Rab34-gRNA-mouse-5'	CACCGATATCCAAGGTCATCGTTGT

Rab34-gRNA-mouse-3'	AAACCTCCGATGGTAGCCTTGTAAC
Rab8A-sequence-5'	CTCTGCACTGCTCCCATCA
Rab8A-sequence-3'	TTCTGGAGAAAGCCCCATGT
Rab8B-sequence-5'	GCAGGTCTTTTATCCGCTGG
Rab8B-sequence-3'	CTTTCCCCGTCCCCTAGTAC
Rab10-sequence-5'	AAGAAGACGTACGACCTGCTTTTCA
Rab10-sequence-3'	CCTTAAAAATATCACACATCTACTAATTCC
Rab11B-sequence-5'	ACTTCTGCACCACTTAGCACAGTGCCTGCA
Rab11B-sequence-3'	CTCCCCTTCTCCTGCCCAACTCCTACACAT
Rab12-sequence-5'	CTACTGCGGAGTAGCTGCTTCCCTTCCTCC
Rab12-sequence-3'	GGAGGAAGGGAAGCAGCTACTCCGCAGTAG
Rab34-sequence-5'	TCCTCTCTTTGTTGTGGGTGTCCCTAACTC
Rab34-sequence-3'	GGCCCCGGGTGATTGTTTCATCTCCGTGGC
Rab34-sequence-mouse-5'	GGGGAGGAGTGACAGACAGA
Rab34-sequence-mouse-3'	GACTTCCTGCATTCCAGAGC
DonorBFP-sequence	GTTGTCCACGGTGCCCTCCATGTAC

siRNA Name	Sequence
siCEP164	TCAAGGCCCRGGAAGATAT
siRab1A	CCACAAAGAAAGTAGTAGA
siRab1B	TGACGTCACTGACCAGGAA
siRab2A	TGACCTTACTATTGGTGTA
siRab2B	GTTCCAACATGGTTATCAT
siRab3A	AGGACAACATTAACGTCAA
siRab3B	CCAATGAAGAGTCCTTCAA
siRab3C	CAGTTGGGATCGATTTCAA
siRab3D	GGACGAACGTGTTGTGCCT
siRab4A	GGACCTGGATGCAGATCGT
siRab4B	GCCCCAACATCGTGGTCAT
siRab5A	GTCCGCTGTTGGCAAATCA
siRab5B	AGACAGCTATGAACGTGAA
siRab5C	ACGAAATCTTCATGGCAAT
siRab6A	GGAGCTTGATTCCTAGCTA
siRab6B	CCATTGGGATTGACTTCTT
siRab6C #2	CCTTTTCCCTTCATTAATA
siRab6C #1	ATCATCACGCTAGTAGGAAA
siRab41/6D	GGAGCGCTTTCACAGCCTA
siRab7	CCATTGGGATTGACTTCTT
siRab7B/42	AGGCTGGTGTAGAGAGAAA
siRab8A	CCATAGGAATTGACTTTAA
siRab8B	TGACAAAACTCAACAGAAA
siRab9A #1	GGAAGCGGTTCGAAGAGTT
siRab9A #2	GCCCAAGCCTAGCTCATCT
siRab9B	GCAGGGTCTTCGTGCTGTT
siRab10 #2	GGAATAGACTTCAAGATCA
siRab10 #1	CTACCTTTATTTCCACCAT

siRab11A	AGAGCGATATCGAGCTATA
siRab11B #1	GCAACATCGTCATCATGCT
siRab11B #2	AGAACAACTTGTCCTTCAT
siRab12 #3	AGGAATGAGTTGTCCAATA
siRab12 #2	CCGTGGGTGTTGACTTCAA
siRab13	TGAGAAATCTTTCGAGAAT
siRab14	ATGGCTTATTGTTCCTCGA
siRab15	CCATCACAAAGCAGTACTA
siRab17	GGAAGGATTCCTTCCTCAA
siRab18	TCCAGAACTTGCAGCAACA
siRab19	TCTGCCAAGGAGTCAAAGA
siRab20	GTGGATATATCCAGTCATA
siRab21	GGAACTCTTTCTTGACCTT
siRab22A	GAAGAGACATTTTCAACAT
siRab22B	AGTGCGACCTCTCAGATAT
siRab23	GAACATCAGTGAAAGAAGA
siRab24	GAGGAGGGCTGCCAAATCT
siRab25	CCAATCTACTCTCCCGATT
siRab26	GGCATTGACTTCCGGAACA
siRab27A	CCAGTGTACTTTACCAATA
siRab27B	GCAAATGCTTATTGTGAAA
siRab28	AGGCAGATATTGTAAACTA
siRab29	TGAGAGTCCTCATTGAAAA
siRab30	GCAACAAGGTCATCACTGT
siRab32	CCAAAGCTTTCCTAATGAA
siRab33A	AAAGCATGGTCGAGCATTA
siRab33B	AGAGCATGGTTCAGCACTA
siRab34 #3	TGCATTGCATCAACCTACT
siRab34 #1	AGACACCTTTGATAAGAAT
siRab35	GCAGTTTACTGTTGCGTTT
siRab36	GCCCCAGCTTTCACAGCCA
siRab37	CATGTTTCCTGATCCAATT
siRab38	AGCACATACTTGCAAATGA
siRab39A	CCGACGATCTTTTGAACAT
siRab39B	GAGAGGAGATGTTTGTGCT
siRab40A #2	GCCTCTGCAAAGTGGAGAT
siRab40A #1	GAGCCTGCAGGATGGTGCA
siRab40B #1	CGGCATTGATCGATGGATT
siRab40B#2 (simRab40B)[#]	CAGCTGCAAAATTTCTTAGTT
siRab40C	AGAACTGCATGACCTTCTT
siRab42/43 #1	CCAGGTCCTTTTACCGGAA
siRab42/43 #2	GGAAGTCCTTTGAACACAT
siRab43/41 #1	CCATGAAGACGCTGGAGAT
siRab43/41 #3	AGCGGGTCAAGCTGCAGAT
siRILP	GGAGCGGAATGAACTCAAA
siFLCN #1	GAAGCTCGCTGATTTAGAA

siFLCN #2	CCATCATGATGGACCGGAT
siMunc13-2	TCACACTCATCGTGTCAAT

[#]simRab40B (siRNA against mouse Rab40B) was originally reported in Matsui and Fukuda (2013). It was effective for human Rab40B, because its target sequence is also conserved in human Rab40B

Acknowledgements

I achieved this thesis in Laboratory of Membrane Trafficking Mechanisms, Integrative Life Sciences, Graduate School of Life Sciences, Tohoku University. I am most grateful to Professor Mitsunori Fukuda for giving me a chance and appropriate guide to perform research of membrane trafficking mechanism. I am also very thank Yuta Homma and Takahide Matsui for teaching me the experimental methods and giving me helpful advice. I wish to express my deep gratitude to Megumi Takada-Aizawa and Kazuyasu Shoji for thchnical assistances, to Michi Tani for kindness support, and to all members of the laboratory for valuable discussions and advices.